AWARD NUMBER: W81XWH-15-1-0658

TITLE: Novel Cyclic Lipopeptides for Treating Complicated Wound Infections

PRINCIPAL INVESTIGATOR: Stephen C. Davis

CONTRACTING ORGANIZATION: University of Miami Miller School of Medicine

REPORT DATE: Dec 2019

TYPE OF REPORT: Final

PREPARED FOR: U.S. Army Medical Research and Materiel Command
Fort Detrick, Maryland 21702-5012

REPORT DOCUMENTATION PAGE

Form Approved
OMB No. 0704-0188

1. REPORT DATE	2. REPORT TYPE	3. DATES COVERED
Dec 2019	Final	09/21/2015 - 09/20/2019

4. TITLE AND SUBTITLE
Novel Cyclic Lipopeptides for Treating Complicated Wound Infections

5a. CONTRACT NUMBER

5b. GRANT NUMBER
W81XWH-15-1-065

5c. PROGRAM ELEMENT NUMBER

6. AUTHOR(S)
Stephen Davis

E-Mail: sdavis@med.miami.edu

5d. PROJECT NUMBER

5e. TASK NUMBER

5f. WORK UNIT NUMBER

7. PERFORMING ORGANIZATION NAME(S) AND ADDRESS(ES) AND ADDRESS(ES)
University of Miami Miller School of Medicine
ATTN: JILL TINCHER
1400 NW10 AVE RM 1007P
MIAMI FL 33136-1002

8. PERFORMING ORGANIZATION REPORT NUMBER

9. SPONSORING / MONITORING AGENCY NAME(S) AND ADDRESS(ES)
U.S. Army Medical Research and Materiel Command
Fort Detrick, Maryland 21702-5012

10. SPONSOR/MONITOR'S ACRONYM(S)

11. SPONSOR/MONITOR'S REPORT NUMBER(S)

12. DISTRIBUTION / AVAILABILITY STATEMENT
Approved for Public Release; Distribution Unlimited

13. SUPPLEMENTARY NOTES

14. ABSTRACT
The purpose for this grant was to develop a new class of antibacterial agents, cyclic lipopeptides, derived from the fusaricidin/LI-F family of naturally occurring antifungal antibiotics for the prevention and treatment of complicated combat-related or trauma-induced wound infections caused by multidrug-resistant (MDR) pathogens and biofilm formation. Three aims were planned: (1) To optimize/synthesize lead cyclic lipopeptides and assess their antimicrobial/antibiofilm activity and toxicity *in vitro*; (2) to develop and optimize a cyclic lipopeptide delivery system based on anionic graft copolymer nanoparticles for topical application; and (3) to characterize/optimize, evaluate dosing, efficacy, and toxicity/safety of the combined cyclic lipopeptide/polymer nanocomplexes in several porcine models for infection prevention, biofilm elimination, and wound healing. The modification of the amino acid sequences of lead depsipeptides were designed to disrupt the balance between the charge and hydrophobicity leading to a better separation of antibacterial activity and nonselective toxicity. In vitro and in vivo studies were performed to study antimicrobial and wound healing efficacy.

15. SUBJECT TERMS
Antimicrobial peptides, *Pseudomonas aeruginosa,* Burn Wounds, Healing

16. SECURITY CLASSIFICATION OF:			17. LIMITATION OF ABSTRACT	18. N	19a. NAME OF RESPONSIBLE PERSON
a. REPORT	b. ABSTRACT	c. THIS PAGE			19b. TELEPHONE NUMBER *(include area code)*
Unclassified	Unclassified	Unclassified	Unclassified		USAMRMC

Table of Contents **Page No.**

1. Introduction

The purpose of this grant was to develop a new class of antibacterial agents, cyclic lipopeptides, derived from the fusaricidin/LI-F family of naturally occurring antifungal antibiotics for the prevention and treatment of complicated combat-related or trauma-induced wound infections caused by multidrug-resistant (MDR) pathogens and biofilm formation. Three aims were planned: (1) To optimize/synthesize lead cyclic lipopeptides and assess their antimicrobial/antibiofilm activity and toxicity *in vitro*; (2) to develop and optimize a cyclic lipopeptide delivery system based on anionic graft copolymer nanoparticles for topical application; and (3) to characterize/optimize, evaluate dosing, efficacy, and toxicity/safety of the combined cyclic lipopeptide/polymer nanocomplexes in several porcine models for infection prevention, biofilm elimination, and wound healing. The study hypothesis was that modification of the amino acid sequences of lead depsipeptides would disrupt the balance between the charge and hydrophobicity leading to a better separation of antibacterial activity and nonselective toxicity. Both *in vitro* and *in vivo* studies were performed to evaluate the efficacy of the topical formulations.

2. KEYWORDS:

Antimicrobial peptides, Infection, Biofilms, *Pseudomonas aeruginosa,* Wounds, Healing

3. ACCOMPLISHMENTS:

a) Major goals and objectives

Specific Aim 1: Optimize lead cyclic lipopeptides using systematic and rational synthetic chemistry approach.
Major Task 1: Optimize amino acid sequence of lead cyclic lipopeptides.
Subtask 1: Obtain the University of Miami Institutional Animal Care and Use Committee (IACUC) and ACURO approval for the use of porcine model in the proposed in vivo experiments.
Subtask 2: Synthesize unusual amino acid building blocks.
Subtask 3: Synthesize cyclic lipopeptides with different amino acid sequences.
Subtask 4: Assess synthesized peptides in vitro antimicrobial/antibiofilm activities and toxicity.
Major Task 2: Optimize the lipidic tail of the lead cyclic lipopeptides.
Subtask 1: Synthesize cyclic lipopeptide with optimized lipidic tail length and intercharge distance.
Subtask 2: Assess synthesized peptides in vitro antimicrobial/antibiofilm activities and toxicity.
Major Task 3: Large scale synthesis and purification of selected cyclic lipopeptides.
Subtask 1: Synthesize and purify large gram quantities of selected cyclic lipopeptides required for research outlined in Aims 2 and 3.

Specific Aim 2: Develop and optimize cyclic lipopeptide delivery system for topical application.
Major Task 4: Synthesize graft copolymers and their cyclic lipopeptide nanocomplexes.
Subtask 1: Validate synthesis protocol for graft copolymers from PMAA and PPAA backbones and polyetheramines at 1g/batch scale.
Subtask 2: Prepare cyclic lipopeptide/polymer nanocomplexes with various peptide/polymer charge ratios and peptide concentrations.
Major Task 5: Characterize properties of cyclic lipopeptide/polymer complexes.
Subtask 1: Assess efficacy of nanocomplex binding and release kinetics for cyclic lipopeptide using ultrafiltration, dialysis and RPHPLC.
Subtask 2: Determine stability of cyclic lipopeptide/polymer nanocomplex in human plasma using RP-HPLC and MALDI-TOF MS.
Subtask 3: Optimize the viscosity of the cyclic lipopeptide/graft copolymer nanocomplex formulations for topical delivery
Major Task 6: Assess antimicrobial activity and toxicity of cyclic lipopeptide/polymer nanocomplexes.
Subtask 1: Assess cyclic lipopeptide/polymer complexes in vitro antimicrobial/antibiofilm activities and toxicity.
Subtask 2: Based on the data from Aims 1 and 2, prepare optimal selected cyclic lipopeptide/polymer formulation in large quantity.
Specific Aim 3: Assess selected cyclic lipopeptides therapeutic potentials using porcine wound infection model.

Major Task 7: Evaluate therapeutic potential of lipopeptides in porcine partial thickness wound infection model
Subtask 1: Assess efficacy of selected lipopeptides using deep partial thickness infection prevention model.
Subtask 2: Assess efficacy of lipopeptide/polymer nanocomplexes using deep partial thickness infection prevention model.
Subtask 3: Assess effects of lipopeptides on bacterial virulence in vivo
Major Task 8: Assessment of lipopeptides anti-biofilm potential in vivo using full thickness biofilm elimination model.
Subtask 1: Assess efficacy of selected lipopeptides and lipopeptide/polymer nanocomplexes in porcine full thickness biofilm-associated elimination model.
Major Task 9: Effects of lipopeptide formulations on wound healing
Subtask 1: Assess effects of selected lipopeptides and lipopeptide/polymer nanocomplexes on wound healing.
Subtask 2: Histological and visual assessment of wound tissue.
Subtask 3: Molecular assessment of wound tissue.

b) Accomplishments under the goals

Along with Torrey Pines we have accomplished the following:

1. Obtained the IACUC and Animal Care and Use Review Office (ACURO) approval
2. We published the following publication: N. Bionda, R. M. Fleeman, C. de la Fuente-Núñez, M. C. Rodriguez, F. Reffuveille, L. N. Shaw, I. Pastar, S. C. Davis, R. E.W. Hancock, P. Cudic, Identification of novel cyclic lipopeptides from a positional scanning combinatorial library with enhanced antibacterial and antibiofilm activities, *Eur J Med. Chem.* 2016 Jan 27;108:354-63.doi:10.1016/j.ejmech.2015.11.032
3. Submitted an abstract entitled “Tryptophan and arginine rich antibacterial cyclic lipopeptides” for the 2016 MHSRS meeting.
4. Completed Major Task 1, Subtasks 1 and, 3
5. Completed Major Task 1, Subtasks 2 and 4
6. Completed Major Task 2, Subtasks 1 and 2
7. Completed Major Task 3
8. Completed Task 4-6 (Synthesize graft copolymers and their cyclic lipopeptide nanocomplexes). Due to Torrey Pines subcontract (Dave Davore: Rutgers) running out of money to complete this task, we have continued work with a DMSO delivery system.
9. Presented at the 28th Annual Meeting of the Wound Healing Society with the Symposium on Advanced Wound Care (SAWC). Georgia World Congress Center in Atlanta, Georgia, April 13-17, 2016
10. Completed Task 7-9
11. Presented at the Military Health System Research Symposium, Kissimmee, FL, August 19-22, 2019

Significant Results and Key Outcomes

Major Tasks 1-3 (see report from partnering PI, Richard Houghten [Torrey Pines])
Work completed by Dr. Houghten (10/1/2018-10/1/2019)

Both the cationic nature and amphipathicity are the key factors in the core sequences in this study that drive antibacterial activity. We have carried out residue-specific modifications of existing cyclic antimicrobial peptides for peptide lead optimization. The Cyclic lipopeptide **1** (CLP1 **Figure 1**) was synthesized and purified. It displayed antibacterial activity against *Enterococcus faecium* (USF-14489), *Methicillin resistant S.aureus* (CBD-635) *and A.baumannii* (USF-1403) in accordance to the protocol recommended by the Clinical and Laboratory

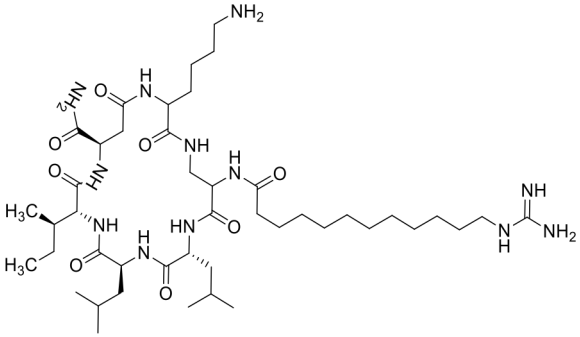

Figure 1. Structures of cyclic lipopeptide1 (CLP1)

Standards Institute (CLSI). Literature suggests that the net positive charge enhances the interaction with anionic lipids and other bacterial targets leading to improved antibacterial activity. To explore the effect of chain length on antimicrobial activity, we chose to compare tails having 6, and 12 carbons between the acid and functionalized lipid terminal. In our previous studies we reported the synthesis of 26 analogs with varying lipid tail lengths C-6 and C-12 respectively along with 12 different tail heads using the guanido head reported previously as a control series. Using CLP-1 as a model we have in the past synthesized 26 analogs analogs with C-6 and C-12 tails. The parent series **2569** was reported in 2017- first quarter. These syntheses enabled the determination of effects of the tail length on the antibacterial activity. Also, we synthesized 12 different tail head (X 1-12) modifications by replacing the guanido head with various urea derivatives using a range of isocyanates purchased from Sigma-aldrich. We observed that the C-12 tail length was more potent against *Staphylococcus aureus* Mu50 (MRSA) ATCC 700699, *Escherichia coli* K-12 ATCC 29181, and *Acinetobacter baumannii* ATCC 19606 than the respective C-6 tailed counterparts.

The general synthetic approach for the synthesis of the Cyclic lipopeptide analogs was developed and was previously reported by Cudic et al. (Bionda, N.; Fleeman, R.M.; de la Fuente-Núnez. C.; Rodriguez, M.C.; Reffuveille , F.; Shaw, L.N.; Pastar, I.; Davis, S.C.; Hancock , R.E.W ; Cudic, P. *Eur. J. Med. Chem*., 2016 ,**108,** 354-363.)

In short, the macrocycle comprises of Fmoc-D- aspartic acid α-allyl ester, Fmoc-D-isoleucine, Fmoc-L-Leucine, Fmoc-D-leucine, N^{α}–Fmoc-N^{β}-4-methyltrityl-L-2,3-diaminopropionic acid and N^{α}–Fmoc-N^{ε} -Boc- D-lysine (Chemimpex) added sequentially onto the solid support Tentagel RAM resin (RAPP polymere) followed by addition of the lipid tail Fmoc-6-aminohexanoic acid or Fmoc-12-amino dodecanoic acid (Chemimpex) by tea-bag approach. Once the lipid tail is added, the respective isocyanates/guanidine moiety or citrulline were coupled using Standard Solid phase Chemistry to make analogs that have urea tail heads. The cyclization of the lipopeptide was performed on the solid support using (benzotriazol-1-yloxy) tripyrrolidinophosphonium hexafluorophosphate (PyBop), 1-hydroxybenzotriazole (Hobt) and N,N-Diisopropylethylamine (DIEA) in DMF.

The final cyclic lipopeptides were cleaved from the resin using 88% trifluroacetic acid (TFA)/ 6% water/ 6% triisopropylsilane (TIS).

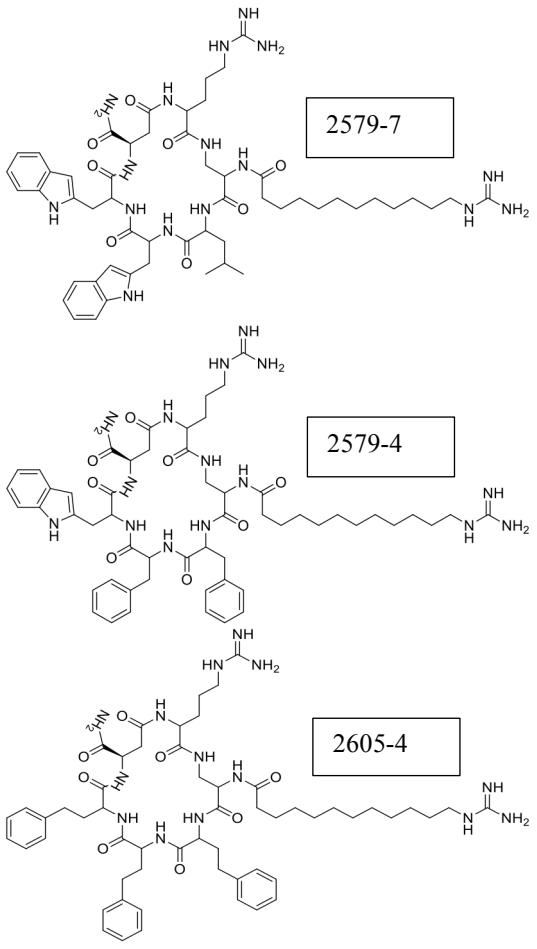

Figure 2. Structures of lead experimental cyclic lipopeptides **2579-7, 2579-4 and 2605-4** synthesized at Torrey Pines.Institute for Molecular Studies

We have synthesized and reported several series of compounds in the past years: namely-**2569**, **2579**, **2589, 2583, 2605, 2612 and 2617**.We narrowed down to two lead cyclic lipopeptides namely **2579-4, 2579-7 and 2605-4** based on their antimicrobial potency. The structures of the lead peptides are shown below in **Figure 2**. The respective peptides were then scaled up and sent to Dr. Davis at Miami school of Medicine, who assessed the ability of cyclic lipopeptides **2579-4** and **2579-7** to reduce the proliferation of MRSA USA300 in the porcine wound model. Both **2579-4, 2579-7** peptides have proven to be effective against partial thickness porcine wound model reported earlier.

Dr. Houghten's lab has mastered the ability to repeatedly scale up the synthesis of the cyclic peptides such as **2579-4**, **2579-7** to yield 300-400mgs of crude peptide (~50-60% purity). Both **2579-4**, **2579-7** was scaled up and pure material (>90% purity) was delivered to Dr. Devore at Rutgers as well as to Dr. S.C Davis at University Of Miami Miller School Of Medicine. Dr. Devore successfully complexed the peptide into a nano-complex hydrogel formulation with a higher concentration of **2579-4 and 2579-7**. The nanoformulated cyclic lipopeptides **2579-4**, **2579-7** reduced the *MRSA* colony forming units (CFU/mL) by 3.67 and 3.78 log units at a low concentration of 7mg/ml (0.7 % loading) as compared to untreated control. Mupirocin (1% cream) was used as positive control **(See Figure 13).** As expected, we have observed an increased reduction in Colony Forming units with increased loading of peptide in the hydrogel.

Progress towards Synthesis of cyclic lipopeptides with unusual amino acid building blocks

The key to the development of potent non–toxic antibacterial agents lies in the ability to balance hydrophobicity and positive charge. Hence, in pursuit of better drug candidates we have introduced hydrophobic as well as unnatural amino acid residues. As of last year we have successfully introduced unnatural amino acids including Fmoc-D-Homophenylalanine, and. Fmoc-L-Homophenylalanine (Major Task 1, Subtask 2) in the macrocycle and achieve potent antimicrobial activity. Last quarter we reported successful synthesis of 16 new compounds–the **2612** series. These molecules have exocyclic residues, such as Fmoc-D-Lys(Boc)-OH, Fmoc-L-Lys(Boc)-additional positive charge and also increased flexibility between the cycle and the tail. This allowed the molecule to freely interact with the bacterial membranes, thus resulting in non-specific broad spectrum activity (**Figure 4**). In this quarter we have successfully scaled up **2612-8, 2612-13 and 2612-16** (**Figure 5**) reported last quarter as they exhibited broad spectrum activity against MRSA, *P.aeruginosa* and *A.baumannii*. The select lead compounds **2612-8, 2612-13 and 2612-16** (**Figure 5**) were scaled up successfully to yield 200-300mgs of crude product. The **2612-8, 2612-13 and 2612-16** are exocyclic modications of the lead compounds **2579-7** and **2605-4** reported previously. They were shipped out this quarter to Dr. S.C.Davis to perform porcine-would healing studies against *P.aeruginosa.*

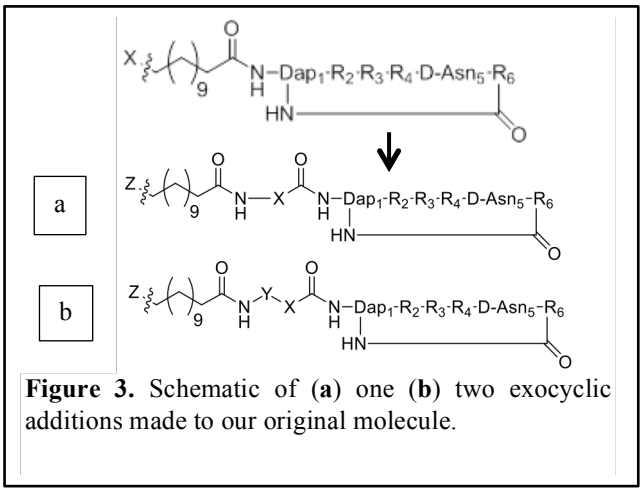

Figure 3. Schematic of (**a**) one (**b**) two exocyclic additions made to our original molecule.

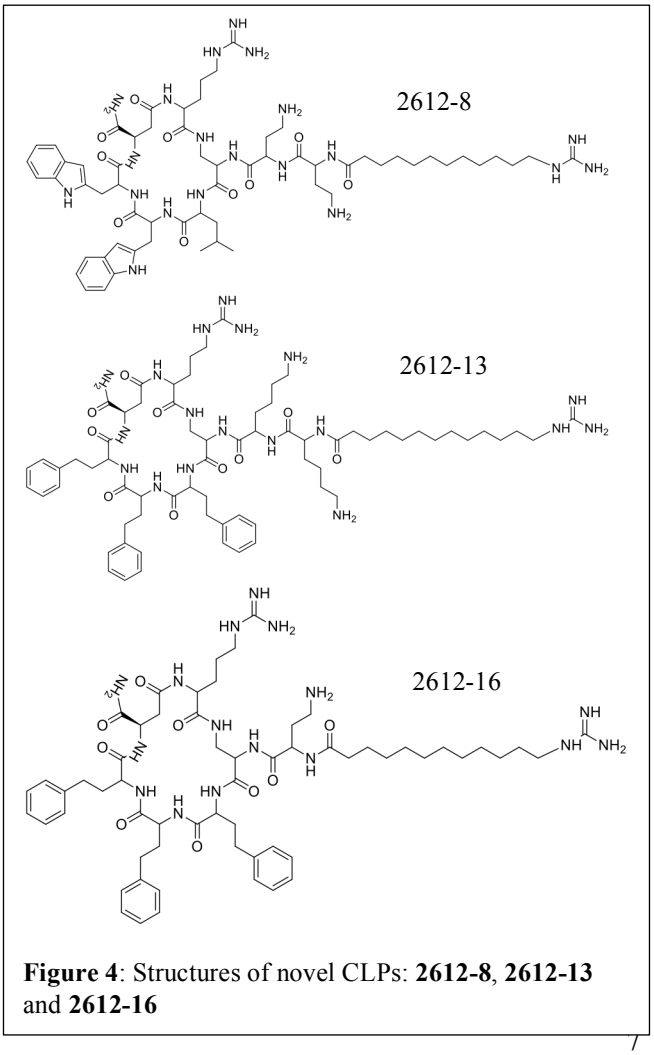

Figure 4: Structures of novel CLPs: **2612-8**, **2612-13** and **2612-16**

There were two versions of **2612-8: 2612-8.1, 2612-8.2** repectively. They only difference being, in **2612-8.1** the two exocyclic residues were L-DAB and in **2612-8.2** the first exocyclic residue was a L-DAB and the second one was D-DAB. We wanted to explore if the sterochemistry of the exocyclic residues played any role in antimicrobial potency and indeed having the two L-DAB exocyclic residues presented better activity against *P.aeruginosa invivo* as shown in **Figure 5**.

The mass of the crude peptide obtained post synthesis was percent yield of crude CLP **2605-4** (Mol wt: 1079.34) was 407.3 mg, resulting in crude percent yield

of 78.6%, which was reduced to ~32% post RP-HPLC. As for the CLP **2612-8.1** (Mol wt:1281.55) was 451.2mg, resulting in the crude percent yield of 73.3%, which was reduced to ~30% post RP-HPLC. The Molecular weights of the Cyclic lipopeptides was confirmed using Shimadzu ESI LC-MS and Bruker MALDI-TOF.

Initial Assessment of Cyclic Lipopeptides and their Antibacterial Selectivity

Antibacterial activities of all the lead new cyclic lipopeptides **2579-4, 2579-7, 2605-4, 2612-8.1, 2612-13 and 2612-16** identified **a**re reported in comparison with Collistin and vancomycin in **Table 1**. We chose Gram-positive and Gram-negative bacterial strains: *Staphylococcus aureus* Mu50 (MRSA) ATCC 700699, and *Acinetobacter baumannii* ATCC 19606, *Pseudomonas aeruginosa* ATCC-27853, respectively. Antibacterial assays were performed in sterile 96-well flat-bottomed polystyrene plates by the standard microdilution broth method using trypticase soy broth (TSB). Controls on each plate were media without bacteria, bacterial inoculum without antimicrobials added, and bacterial inoculum containing vancomycin and collistin. Stocks of microorganisms maintained at -80 ^{o}C in 20% glycerol were thawed and streaked on agar plates as recommended by ATCC protocols for each particular microorganism to isolate single colonies. To perform the broth microdilution assay a single isolated colony was grown in 5mls of fresh media for about 4 hrs. The bacterial suspension was then diluted using fresh media to $10^5 - 10^6$ Colony Forming Units (CFU)/ml. The diluted peptides as well as control antibiotics used in this assay ranged from 3.1-100 µg/mL. All the tests were performed in duplicates and were repeated as two independent experiments. Stock solutions of cyclic peptides were made in 1X PBS. Plates were then loaded with 10 µL aliquots of serial dilutions of the cyclic peptides/controls and 90 µL diluted bacterial suspension. Plates were then incubated at 37^{o}C overnight and after 18 hrs of incubation MIC90s were recorded.

Antibacterial activities of all the lead new cyclic lipopeptides **2579-4, 2579-7, 2605-4, 2612-8.1, 2612-13 and 2612-16** identified **a**re reported in comparison with Collistin and vancomycin in **Table 1**.

Table 1: Antibacterial activities of all the lead new cyclic lipopeptides **2579-4, 2579-7, 2605-4, 2612-8.1, 2612-13 and 2612-16**

Cyclic lipo-peptides	MRSA	*P. aeruginosa*	*A. baumannii*
2579-4	12.5-25	97.43 ± 0.59	25-50
2579-7	21.07 ± 0.13	131.19 ± 2.76	25-50
2605-4	3.1-6.25	ND	6.25-12.5
2612-8.1	12.5-25	12.5-25	6.25-12.5
2612-13	6.25-12.5	6.25-12.5	6.25-12.5
2612-16	6.25-12.5	12.5-25	<6.25
Colistin	>100	ND	<0.78
Vancomycin	12.5-25	ND	>100

The data suggests that the CLP **2605-4** with hydrophobic unnatural amino acid (homophenylalanine) in the macrocycle was the most effective against Gram-positive *Staphylococcus aureus* Mu50 (MRSA) ATCC 700699, MIC 90: 3.1-6.25 µg/mL. It was also effective against *Acinetobacter baumannii* ATCC 19606 with an MIC 90 of 6.25-12.5 µg/mL. Whereas the CLP's with the two cationic exocyclic residues (diaminobutyric acid), **2612-8.1, 2612-13 and 2612-16** proved to be efficacious against *Pseudomonas aeruginosa* ATCC-27853 and had comparable efficacy to that of **2605-4** against *Acinetobacter baumannii* ATCC 19606, MIC 90 of 6.25-12.5 µg/mL (**Table 1**). The lowest *P.Aeruginosa* counts were found in wounds that were treated with peptide **2612-8.1** *invivo* at 20 mg/ml (6.18 log CFU/g-see **Figure 14**). The addition of hydrophobic unnatural amino acids to the macrocycle lead to increased efficacy against Gram-positive bacteria whereas addition of positively charged exocyclic residue- diaminobutyric acid lead to similar or increased activity against Gram-negative bacterial strains. We hypothesize that addition of above exocyclic residues added additional positive charge and increased flexibility between the macrocycle and

the tail. This allowed the molecule to freely interact with the bacterial membranes, thus resulting in non-specific broad-spectrum activity.

Work completed by collaborator D. Devore at Rutgers University, (Subcontract) Major tasks 4-6

We report here on work directed at the formulation and characterization of "GRAPLON" graft polyelectrolyte surfactant (PS) nanocomplexes of Torrey Pines Institute for Molecular Studies (TPIMS) antimicrobial cationic cyclic lipopeptides (CLPs) and the formulation and characterization of those GRAPLON CLPs into biopolymer hydrogel matrixes for use in porcine infected wound studies which were conducted at the University of Miami.

Methods

Graft polyelectrolyte surfactant synthesis. The graft polyelectrolyte surfactants (PS) were comprised of a poly(methacrylic acid) (PMAA) backbone with nominal 1mol%, 5 mol% and 10 mol% grafted pendent polyetheramine Jeffamine M-2070^{TM} (Huntsman Corp., The Woodlands, TX) and were abbreviated as PMAA-g-x%J, where x=1,5, or10 (Figure 1). Jeffamine M2070 is a primary amine-terminated random copolymer of ethylene oxide (EO):propylene oxide (PO) with EO:PO molar ratio of 31:10 and a molecular weight of 2 kDa.

The PMMA backbone was synthesized as using free radical polymerization of methacrylic acid monomer with AIBN as the radical initiator. Dry yield of the polymer was approximately 90%. The PMAA molecular weight distribution was characterized via gel permeation chromatography (GPC). The GPC system consisted of a 515 HPLC pump, 717plus auto sampler, a 2414 RI detector and Empower Pro® Software (Waters Corporation, Milford, MA). DMF containing 0.1% TFA at a flow rate of 0.8 mL/min was used as the mobile phase. The molecular weights were computed against polystyrene standards, and PMAA composition was confirmed by ^{1}H-NMR (500 MHz-Varian Inova, Santa Clara, CA).

The graft polyelectrolyte surfactants (PSs) were synthesized by carbodiimide coupling and illustrated in **Figure 5.** Briefly, PMAA, anhydrous 1-hydroxybenzotriazole (HOBt) (0.7 mmol), and Jeffamine M-2070 were dissolved in dry dimethylformamide (DMF) at room temperature, N,N-diisopropylcarbodiimide (DIPC) (0.7 mmol) was added and the reaction mixture stirred at 50°C for 30 h. DMF was removed using a Rotavap, the polymer was dissolved in methanol (30 mL) and precipitated in 100 mL diethyl ether. The polymer was filtered through a Buchner filter with fritted disk, allowed to air dry for an hour and then placed under vacuum for 24h to further dry the sample. ^{1}H-NMR (DMSO-d_6-500MHZ) was used to determine the experimental graft density from the ratio of the area under the CH_2CH_2 peak of Jeffamine to the area under the CH_2 peak of the backbone PMAA chain. Molecular weight was determined by GPC.

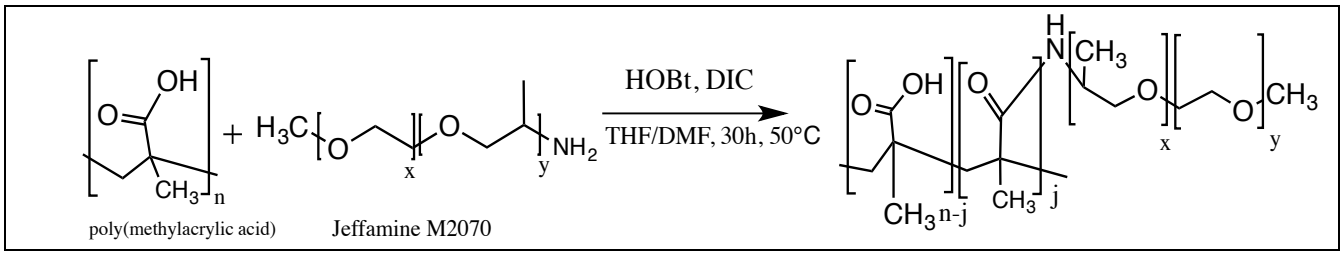

Figure 5. Synthesis scheme for polyelectrolyte surfactant PMAA-g-x%J.

Cytotoxicity assays. The cytotoxicity of the PSs were determined by alamarBlue^{TM} assays of human dermal fibroblast and human primary lung cell cultures run in triplicates. The cells were grown in DMEM cell culture medium in 96-well microtiter plates at 10^4 cells/well. Serial dilutions of the PS were added to each well, and the plates were incubated for 24 h at 37^{o}C. The wells were then rinsed with complete DMEM, 10% alamarBlue in DMEM was added, and the fluorescence intensities were measured with a fluorescent plate reader (Tecan Infinite 200M).

Self-assembly and nanoparticle characterization of PS-CP nanocomplexes. The solubilities of the TPIMS cyclic lipopeptides (CPs) in deionized water (DI H_2O), dimethylsulfoxide (DMSO) and DMSO:H_2O mixtures were evaluated by the presence or absence of visible turbidity. Because of the CPs low aqueous solubilities, nanocomplexes of the CPs with the PS (PMAA-g-10% J) were formed by first combining 50 µL of the CPs at 8.5 mg/mL in DMSO with 50µL of the PS (PMAA-g-10%J) at 5 mg/mL in DMSO and incubating the mixture at room temperature for 30 minutes. These 100 µL DMSO solutions were then added dropwise into 900µL DI water with mixing. The particle sizes and zeta potentials of the resultant self-assembled PS-CP nanocomplexes were then determined by dynamic light scattering and electrophoretic mobility, respectively, using a Malvern ZetaSizer Nano ZS90 (Malvern Instruments, UK) instrument.

Peptide binding levels. The concentration of the peptides in aqueous solutions was obtained by high performance liquid chromatography (HPLC) using a Waters 2695 Separations Module, Waters 2489 UV/Visible Detector, Empower software, and Symmetry Shield RP 18 Analytical Column (3.5 µm diameter silica beads, 2.1 mm × 50 mm). Column conditions were: 25 °C, 10 µL injection volume, 0.5 mL/min flow rate and 6 min run time. The detection wavelength was 215 nm. The mobile phases were: A:HPLC water with 0.1% trifluoroacetic acid; and, B:acetonitrile with 0.1% trifluoroacetic acid. Linear HPLC calibration plots were obtained for known peptide concentrations made by serial dilutions of stock peptide solutions. The binding efficiency of the polyelectrolyte nanocomplexes was measured by ultra-centrifugation of 300µL of self-assembled nanocomplexes made by direct addition of known weight ratios of PS and peptide to deionized water. The nanocomplexes were subjected to ultracentrifugation for 3h at 18°C and 65,000 rpm using a Beckman L8-70M ultracentrifuge (Beckman Coulter, Fullerton, CA). The supernatants were aspirated, directly injected into the HPLC to measure the amount of unbound peptide; the amount of bound peptide was then calculated by subtracting the amount of unbound from the initial loading.

Topical hydrogel formulation and controlled peptide release.
Hydrogel formulations were prepared for topical application of the PS-CP nanocomplexes by direct addition of dry hydroxyethylcellulose (HEC) to the 45:55 DMSO:H_2O solutions of PS-CP's at room temperature. The HEC concentration was adjusted using shear-dependent viscosity measurements to achieve a slightly tacky gel comparable to commercial hydrogel wound dressings. For the porcine partial thickness wound studies, 5mL batches of PS-CP4 hydrogel and PS-CP7 hydrogel containing 7 mg/mL CP were prepared and packaged in calibrated 1 mL glass syringes. 5mL of "control hydrogel" containing only the PS were also prepared and packaged in calibrated 1mL glass syringes. Controlled release of the CPs from the hydrogels was determined by membrane dialysis with the hydrogels (1.0 mL) placed in Spectra/Por 4 dialysis bags submersed in 150 ml of deionized water in a 37°C bath; at selected time points a hydrogel sample was removed from the bag and the amount of the CP's remaining was determined by HPLC.

Antimicrobial activity in vitro assays. The minimum inhibitory concentrations (MICs) of the PS-CAPs were determined against three clinically relevant methicillin-resistant isolates, *Staphylococcus aureus* subsp. aureus Rosenbach ATCC® 700699 (MRSA 600699), *Staphylococcus aureus* subsp. aureus Rosenbach ATCC® BAA-1717 (MRSA USA300) and *Staphylococcus aureus* subsp. aureus Rosenbach ATCC® BAA-1720 (MRSA 252) using the Clinical and Laboratory Standards Institute guidelines for serial broth dilution in polystyrene 96-well plates run in triplicates and the optical density in each well was read at 600 nm wavelength.

The minimum biofilm eradication concentrations (MBECs) were determined following an established high-throughput polystyrene microtiter 96-well plate assay with MRSA USA300 and MRSA 252. Briefly, MBECs were obtained by pre-forming biofilms in 96-well plates by first inoculating each well with $1x10^6$ CFU in TSB, incubating at 37°C for 48h and then gently washing the biofilms two times with PBS. Serial dilutions of the PS-CAPs in water were then added to 2x TSB in the biofilm-containing wells and the 96-well plates were incubated for 24 hr. The wells were then gently washed twice with PBS, 20 µM resazurin (alamarBlue®) was added to each well and the absorbances were obtained with a Perkin-Elmer microplate reader.

Results

Graft polyelectrolyte surfactant syntheses. ^{1}H-NMR (DMSO-d_6-500MHZ) spectra confirmed the PMAA structure and GPC data were indicative of an inverse relationship between the amount of AIBN initiator used and the resultant PMAA molecular weight (**Table 2**).

Table 2. Effect of AIBN molar ratio on PMAA molecular weight

Reaction No.	Monomer	Molar equiv. AIBN	PMAA Mn (kDa)	PMAAMw (kDa)	PDI
1	MAA	0.002	222	753	3.4
2	MAA	0.003	91.6	265	2.9
3	MAA	0.005	7.5	7.5	1.0

Multiple iterative syntheses were performed to demonstrate the reproducibility of the reaction process. A selected PMAA sample having a Mw of 311 kDa and Mn of 148 kDa was then used to prepare graft copolymers with Jeffamine M-2070 pendent chains at selected graft densities. Slight excess amounts of Jeffamine were used in the reaction to achieve a targeted graft density. After grafting, the ^{1}H-NMR spectra had all of the PMAA peaks and additional peaks at s2.9-3.0 ppm (N-CH of Jeffamine) and m3.4-3.7 ppm (CH_2 of Jeffamine). The experimental grafting percentage was calculated by the area ratio of the CH_2 peak of Jeffamine to the CH_2 peak of the PMAA backbone. The experimental graft densities determined by NMR and the GPC molecular weights were summarized in **Table 3**.

Table 3. PMAA-g-x%J graft copolymer properties

Sample (x% targeted graft density)	Mn (kDa)	Mw (kDa)	PDI	Graft density (mole% by NMR)
PMAA (ungrafted)	148	311	2.1	-
PMAA-g-1%J	195	373	1.9	1.0
PMAA-g-5%J	154	171	1.1	4.6
PMAA-g-10%J	147	220	1.5	12

Physical properties of PS-CLP nanocomplexes. In preliminary studies of the nanocomplexes of the experimental cyclic lipopeptide CLP-1 with the PS, PMAA-g-10%J, the particle sizes were found to be independent of the charge ratios (i.e., the amount of bound CLP-1) and the zeta potentials increased (became more positive) as the charge ratio (amount of the added cationic CLP-1 peptide) increased (**Table 4**).

Table 4. Particle size and zeta potential as a function of charge ratio for PS (PMAA-g-10%J)/CLP-1 nanocomplexes in aqueous solution.

Sample	**Nanocomplex Charge Ratio**	**Particle diameter (nm)**	**Zeta Potential (mV)**
PS- CLP-1	0.5	81 ± 1	-16 ± 1
PS- CLP-1	1.0	78 ± 1	-11 ± 0.7

The CLPs in water were found to display low-to-minimal solubility. CLP 2579-4 (CP4) was soluble at 1mg/mL. CLP 2579-7 (CP7) was not soluble in water at that concentration but was soluble at 0.5mg/mL. To deliver those CLPs in vivo, TPIMS and the University of Miami had previously used dimethylsulfoxide (DMSO) and that was found to effectively solubilize the CLPs at concentrations exceeding 20mg/mL. However, the use of DMSO in pharmaceutical formulations that have been approved for human use by the US FDA has been limited to a maximum of 45% DMSO. Therefore, to form stable GRAPLON CLP nanocomplexes and incorporate those in biocompatible hydrogels for topical wound applications, the

solubility of the PS and PS-CLPs were evaluated in mixed 45%:55% DMSO:water. The resultant PS-CP nanoparticle sizes were all below 200 nm, which was consistent with the size limit considered safe and effective for systemic delivery (**Table 5**). After ultracentrifugation and HPLC analysis, the binding levels of the CLPs CP4, CP7 CP26 and CP29 in the PS-CLP nanocomplexes made with the PS PMAA-g-10%J were found to range from 58% (wt:wt) to 85% (**Table 5**).

Table 5. Particle size, zeta potential and bound CP in PS-CP nanocomplexes

Sample	Peptide [mg/mL]	PS [mg/mL]	Particle Size [nm]	Zeta Potential [mV}	Bound Peptide [wt %]
PMAA	-	0.20	12 ± 1	-2.6 ± 0.9	-
PS	-	0.20	48 ± 1	-2.3 ± 1.4	-
CP26	0.40	-	492 ± 64	16 ± 6	-
CP29	0.40	-	578 ± 48	43 ± 2	-
PS-CP26	0.40	0.20	178 ± 17	20 ± 1	85
PS-CP29	0.40	0.20	160 ± 6	34 ± 1	85
PS-CP4	1.7	0.80	156 ± 27	20 ± 1	58
PS-CP7	1.7	0.80	140 ± 9	19 ± 1	62

PS-CLP nanocomplexes were prepared with the PS PMAA-g-1%J and CLPs 2569-11, 2569-26 and 2569-29 at charge ratios (CRs) of 0.5. and 1.0, where the CRs were calculated as the net cationic charge from the cyclic lipopeptides (in electrostatic equivalents), each taken as +2 equivalents/mole, divided by the net anionic charge of the PSs' carboxylic acid groups, which were assumed to be 67% ionized based on prior studies. It was found that the zeta potentials of all the PS-CLPs were positive at CRs of 0.5 and 1.0 (**Table 6**). The positive zeta potentials at CR 0.5 were surprising given that, at least based on stoichiometry, the nanocomplexes should have a large net negative charge. Also, the particle diameters were found to range from 182 nm to more than 1 micron; the larger particle sizes were indicative of particle coagulation. The CLPs by themselves had particles sizes ranging from 159 nm to 578 nm and all had positive zeta potentials. From these data it was concluded that the electrostatic interaction of the cationic CLPs with the anionic PSs caused coagulation into larger particles. However, there was no clear relationship between the zeta potentials, particle sizes and charge ratios of the nanocomplexes.

Table 6. Zeta potential and size of PS-CLP nanocomplexes**.**

Sample	Charge Ratio [+/-]	Zeta Potential [mV]	Particle Diameter [nm]
2569-11	-	6.3 +/- 4.2	159 +/- 2
2569-26	-	16 +/- 6	492 +/- 64
2569-29	-	43 +/- 2	578 +/- 48
PMAA	-	-7.7 +/- 3.4	tbd
PMAA/2569-11	0.5	5.9 +/- 1.5	1253 +/- 82
PMAA/2569-11	1.0	10 +/- 1.7	1453 +/- 56
PMAA-g-1%J/2569-11	0.5	10 +/- 1.8	1227 +/- 225
PMAA-g-1%J/2569-11	1.0	14 +/- 2.7	1080 +/- 166
PMAA/2569-26	0.5	22 +/- 2.8	280 +/- 2
PMAA/2569-26	1.0	-	-
PMAA-g-1%J/2569-26	0.5	27 +/- 3	264 +/- 3
PMAA-g-1%J/2569-26	1.0	32 +/- 4	182 +/- 3
PMAA/2569-29	tbd	-	-
PMAA-g-1%J/2569-29	0.5	14 +/- 0.4	2684 +/- 620
PMAA-g-1%J/2569-29	1.0	24 +/- 3	365 +/- 7

Controlled release of polymyxin B from GRAPLON nanocomplexes.
Polymyxin B and polymyxin E (colistin) are the only cationic cyclic lipopeptides of any class that are approved for human use by the US Food and Drug Administration (FDA). Here polymyxin B (PB) was used as a model system for preliminary evaluation of the CLPs. Because PB is soluble in water, no DMSO was used in preparation of the PS-PB nanocomplexes. The aqueous solubility of PB is due to it having +6 equivalents of cationic charge as compared to only the +2 equivalents of the fusaricidin CLPs. The controlled release of polymyxin B from "GRAPLON" PS-PB nanocomplexes made with three different polymers, poly(methacrylic acid) (PMAA), PMAA-g-5%J or PMAA-g-10%J, was determined using standard membrane dialysis methods at 37°C. PB concentrations in the dialysate (PBS) were determined by HPLC. All three GRAPLON nanocomplexes produced a rapid initial PB release phase over the first 10 hours followed by a slower release phase that extended for at least 7 days (**Figure 6**). Release of PB was fastest and most complete (>90%) from the PMAA-g-10%J nanocomplex and slowest from the PMAA nanocomplex, with the PMAA-g-5%J nanocomplex producing intermediate rates between the others.

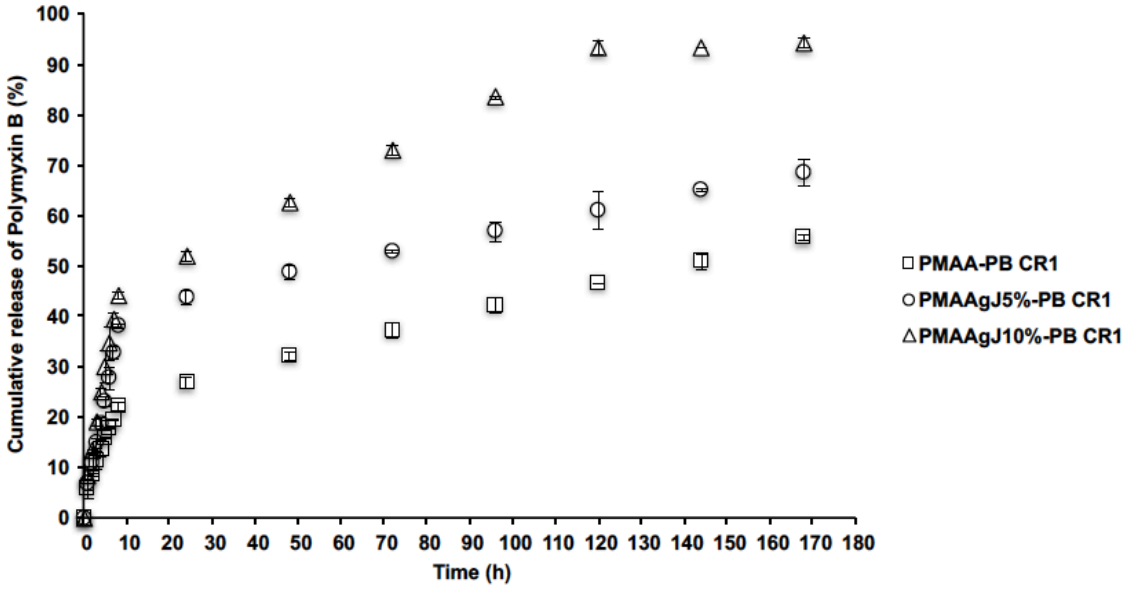

Figure 6. Controlled release of polymyxin B (PB) from GRAPLON PS-PB nanocomplexes of PSs of PMAA (poly(methacrylic acid), PMAA-g-5%Jeffamine M2070 and PMAA-g-10%Jeffamine M2070.

Graft polyelectrolyte surfactant cytotoxicity. The PS, PMAA-g-10%J, was not cytotoxic in vitro to either human dermal fibroblasts (**Figure 7**) or human primary lung cells (data not shown) at concentrations up to 200 µg/mL, whereas the backbone anionic polyelectrolyte PMAA was slightly cytotoxic at 200 µg/mL, which was consistent with prior cytotoxicity results for related anionic graft polyelectrolyte compositions.

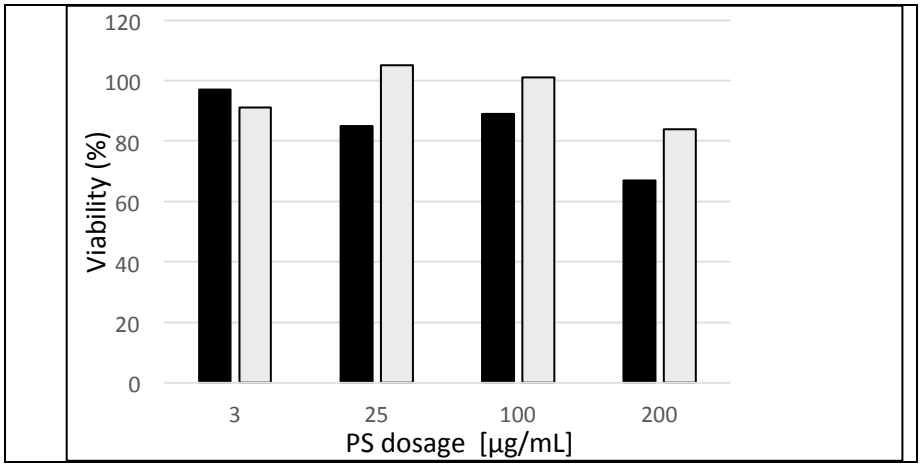

Figure 7. Cytotoxicity of PS (PMAA-g-10%J) and PMAA to human dermal fibroblasts.
Dark bars: PMAA; light bars: PMAA-g-10%J. Data for each bar were the averages of duplicate alamar Blue assays and were normalized against untreated controls.

Antimicrobial and anti-biofilm activities of cyclic lipopeptides and graft polyelectrolyte-peptide nanocomplexes.

The minimum inhibitory concentrations of the CLPs were found to be dependent upon the CLP compositions and the MRSA strain tested (**Table 7**). The impact of the MRSA strain on antimicrobial activity was evident from the substantial difference in the MICs of the positive control vancomycin between MRSA 252 and MRSA USA300. The MIC for vancomycin against MRSA USA300 was consistent with literature values. The PS by itself had no observable antimicrobial activity at concentrations up to 200 μg/mL. The PS-CP nanocomplexes made with the PS PMAA-g-10%J retained significant antimicrobial activity against all strains tested but in most cases the MIC of the PS-CP was approximately one serial dilution concentration level greater than for the corresponding CP by itself. This reduction in antimicrobial activity was consistent with the previously observed behavior of PS nanocomplexes of linear CAPs and was ascribed to the gradual release of the bound CPs from their PS-CP nanocomplexes.

Table 7. MIC's for CPs and PS-CPs against MRSA 252 and MRSA USA300. PS = PMAA-g-10%J

Treatment	MRSA 252 MIC [μg/mL]	MRSA USA300 MIC [μg/mL]
Vancomycin	0.8	12.5
CP4	6.25	12.5
PS-CP4	12.5	25
CP7	12.5	25
PS-CP7	25	25
PS	>200	> 200

Dose-response data for the CLPs and PS-CLPs with PS PMAA-g-10%J against the MRSA biofilms all followed a common pattern of negligible antimicrobial activity up to a critical concentration, at which there was a rapid decrease in microbial viability followed by a high-concentration plateau region of low microbial viability (**Figure 8**). The minimum biofilm eradication concentrations (MBECs) of the CPs and PS-CP nanocomplexes against MRSA biofilms were dependent upon the composition of the CLP and the MRSA strain tested (**Table 8**). The PS by itself appeared to reduce the viability of the MRSA biofilms but, at least at concentrations of up to 400 μg/mL, the PS did not eliminate the biofilms and hence no MBEC values could be assigned.

Table 8. MBECs of CLPs and PS-CLPs

Treatment	MRSA 252 MBEC [μg/mL]	MRSA USA300 MBEC [μg/mL]
Vancomycin	12	50
PS	>400	>400
CP4	12.5	12.5
CP7	12.5	30.0
PS-CP4	25.0	12.5
PS-CP7	25.0	110

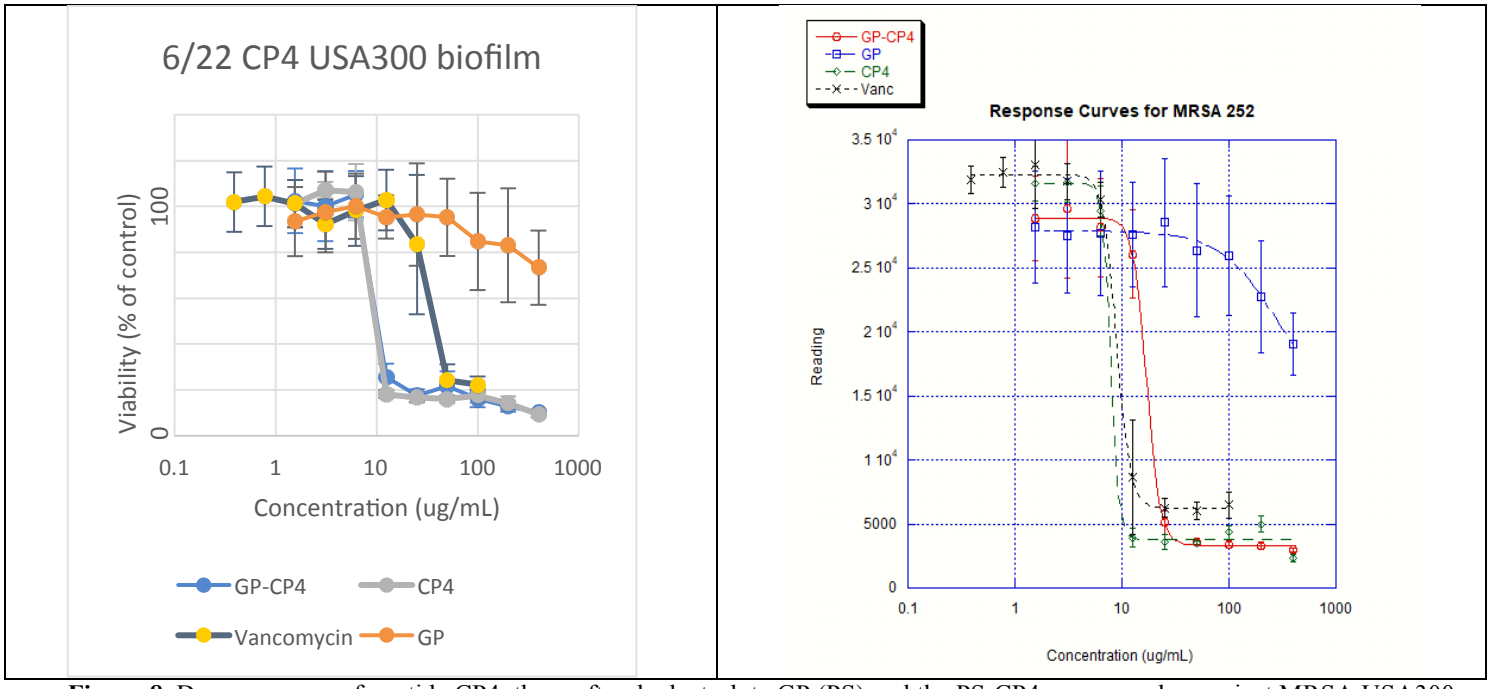

Figure 8. Dose-response of peptide CP4, the graft polyelectrolyte GP (PS) and the PS-CP4 nanocomplex against MRSA USA300 and MRSA 252 biofilms. Vancomycin was used as a positive control.

In vivo antimicrobial activity of GRAPLON hydrogels.

The addition of hydroxyethylcellulose (HEC) to 45:55 (wt:wt) DMSO:H_2O solutions of the CLPs and the PS-CLPs made with the PS PMAA-g-10%J produced optically clear, shear-thinning hydrogels that were slightly tacky to the touch and sufficiently viscous at low shear to allow topical application to wounds without any run-off (**Figure 9**). It was observed that above a CLP concentration of 7 mg /mL in the PS-CPs made in DMSO:H_2O, the solutions became turbid. Consequently, the hydrogels were formulated at maximum CP concentrations of 7 mg/mL, which was significantly less than the 20 mg/mL concentration of the positive control, mupirocin (2%) used in the porcine wound studies.

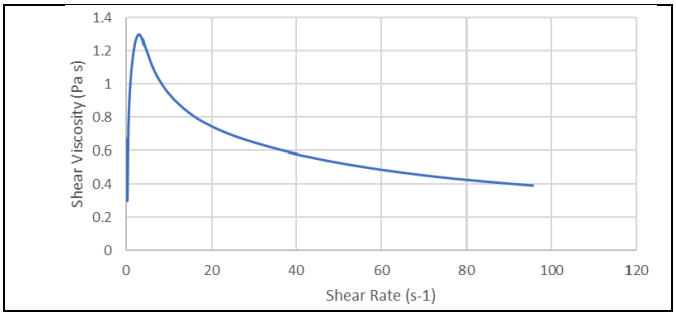

Figure 9. Shear-dependent viscosity of PS-CP7 Hydrogel

The GRAPLON CLP hydrogel formulations made with the PS PMAA-g-10%J and CLPs CP4 and CP7 reduced the microbial populations of porcine partial thickness wounds infected with MRSA USA300 but did not achieve the nearly complete elimination of the infective microbes observed with 2% mupirocin (Refer to **Figure 3**) The GRAPLON CLP hydrogel delivery systems performed more effectively than did the CLPs delivered in DMSO. The significantly better performance of mupirocin was ascribed to its significantly lower MIC against MRSA USA300 (approximately 0.6µg/mL) than the CLPs' MICs, and to the significantly greater concentration of mupirocin (2%) applied compared to the amount of CLP applied (0.7%). Further optimization of the PS-CLP nanocomplexes may enable higher CLP concentrations to be incorporated in the hydrogels.

Summary

The cationic fusaricidin CLPs exhibited structure-dependent antimicrobial MIC activity against both Gram-positive and Gram-negative bacteria. The most effective CLPs against MRSA strains were CP4 and CP7, and these also had relatively low hemolytic activity. The antimicrobial (MIC) and anti-biofilm (MBEC) activities of the CLPs and their GRAPLON CLP nanocomplexes were dependent upon the particular MRSA strain tested. The CLPs and GRAPLON CLPs were more effective than vancomycin against MRSA USA300 biofilms in vitro. Against the MRSA USA300 infections in the porcine partial thickness wounds, the topical hydrogel formulations of the GRAPLON CLPs were significantly more effective than the CLPs delivered in DMSO but were significantly less effective than the 2% mupirocin ointment. The increased performance of the GRAPLON CLP hydrogels containing the PS-CP nanocomplexes was indicative of the value of the PS in enabling significantly higher concentrations of the CLPs to be delivered. Further optimization of the synthetically tunable PSs and CLPs may provide a new tool box of antimicrobial agents for the treatment of wound and burn infections that do not respond to first-line therapies.

Funding for a total of two years (24 months, September 2015-September, 2017) at 0.8 postdoctoral fellow man-years/year for this project was provided to Rutgers University under a subcontract from TPIMS for this project. A no-cost extension and the active participation of Prof. Charles Roth, graduate student Pooja Patel, and Dr. David Devore (co-PI) in the project without funding compensation allowed the subcontract funds to be stretched but all the subcontract funds at Rutgers were finally exhausted in July, 2018. Thus, post July 2108 porcine studies with peptides were carried out using DMSO as vehicle.

In January 2019 TPIMs shipped out 365 mgs of lead compounds **2605-4** and 361 mgs of **2612-8.1** (the last batch of compounds) to the co-partner (Prof. Davis) at the University Of Miami Miller School Of Medicine to complete to complete the full-thickness porcine-model and wound healing studies with the peptides. Since TPIMs had completed all its major tasks, we continued presenting work from our collaborations on **Major tasks 8,9** in the past quarters.

Goals	Percent Completion
Major task 1: Optimize amino acid sequence of lead cyclic lipopeptides	100 %
Major task 2: Optimize the lipidic tail of the lead cyclic lipopeptides	100 %
Major task 3 : Large scale synthesis and purification of selected cyclic lipopeptides	100 %
Major task 4: Synthesize graft copolymers and their cyclic lipopeptide nanocomplexes.	100 %
Major task 5: Characterize properties of cyclic lipopeptide/polymer complexes.	100 %
Major task 6: Assess antimicrobial activity and toxicity of cyclic lipopeptide/polymer nanocomplexes	100 %
Major task 7: Evaluate therapeutic potential of lipopeptides in porcine partial thickness wound infection model	100 %
Major task 8: Assessment of lipopeptides anti-biofilm potential *in vivo* using full thickness biofilm elimination model.	100 %
Major task 9: Assess the Effects of lipopeptide formulations on wound healing	100%

Major Task 7: Evaluate therapeutic potential of lipopeptides in porcine partial thickness wound infection model

Subtasks 1-3: Assess efficacy of lipopeptides using deep partial thickness infection prevention model (prior to biofilm formation) and assessment of lipopeptides on bacterial virulence in vivo.

In these studies, we used our deep partial thickness infection porcine model. We initially assessed three peptides that Torrey Pines found optimal in *in vitro* assays (Peptides: 2365-102/K2R, 2365-102/K2W, 2496-56). We examined each peptide at three concentrations each (2.5 mg/ml, 5 mg/ml and 10 mg/ml). Briefly, deep partial thickness wounds on pigs were inoculated with Methicillin Resistant Staphylococcus aureus (MRSA). After inoculation, wounds were covered with a polyurethane film for 24 hours to allow for biofilm formation. Four wounds were treated twice daily with ~150ul of each formulation. Control wounds were treated with either mupirocin ointment, DMSO vehicle or left untreated (polyurethane film only). On day 4 (post inoculation or day 3 post treatment), wounds were recovered for MRSA quantification using scrub technique and spiral plater system. This technique involves a sterile cylinder being placed over the infected wound area. One mL of scrub solution was pipetted into the glass cylinder and the site was scrubbed with a sterile teflon spatula for 30 seconds. The scrub solution was collected by pipette and stored in sterile glass tubes for transport to the laboratory for enumeration of viable organisms. Serial dilutions were made and colony forming units (CFUs) were quantitated using the Spiral Plater System which deposits a small defined amount of suspension over the surface of a rotating agar plate. Selective media was used to grow MRSA. Colonies on the plates were counted and Log CFU/ml determined.

Figure 10: MRSA counts 3 days after treatment application

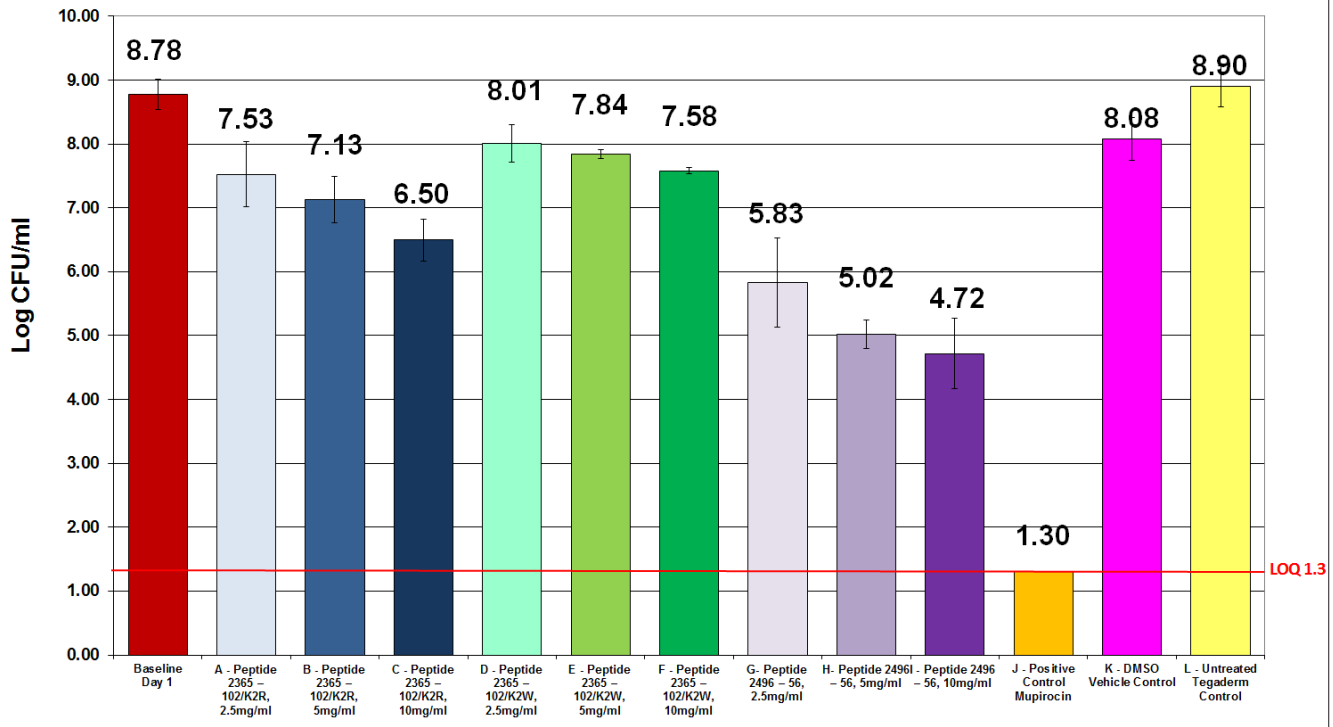

A dose response effect was seen with all three peptides with the highest concentration (10mg) being the most effective (**Figure 10**). The peptide with the greatest reduction of MRSA was Peptide 2496-56. This reduction was over 4 Logs lower than untreated control. The positive control, mupirocin, had completely eliminated the MRSA.

After examining various peptides against MRSA, we were given two new peptides that Torrey Pines found to be more effective against *Pseudmonas aeruginosa* (PA 09-010 – a military isolate obtained with USAISR). Wounds were created as described above and inoculated with *P. aeruginosa*. Sets of wounds

were treated with two peptides (2579-4-2 or 2529-7-2) at two concentrations of each peptide (10mg/ml and 20mg/ml) as compared to DMSO vehicle, Silver Sulfadiazine (SSD) and Tegaderm control (note: all wounds were covered with the polyurethane film dressing, Tegaderm, to keep treatments in place). Wounds were treated daily with the various treatments and on day 3, wounds were recovered using a scrub technique (described above). A selective media for *P. aeruginosa* (Pseudomonas Agar with CN supplement) was used to quantify *P. aeruginosa*. The below results (**Figure 11**) showed that the positive control, Silver Sulfadiazine was the most effective treatment in reducing *P. aerugionsa*. Peptide 2579-7-2 at the higher concentration (20mg/ml) was the second best followed by peptide 2579-4-2 (20mg/ml).

Figure 11: *Pseudomonas aeruginosa* counts after 3 days of treatment application

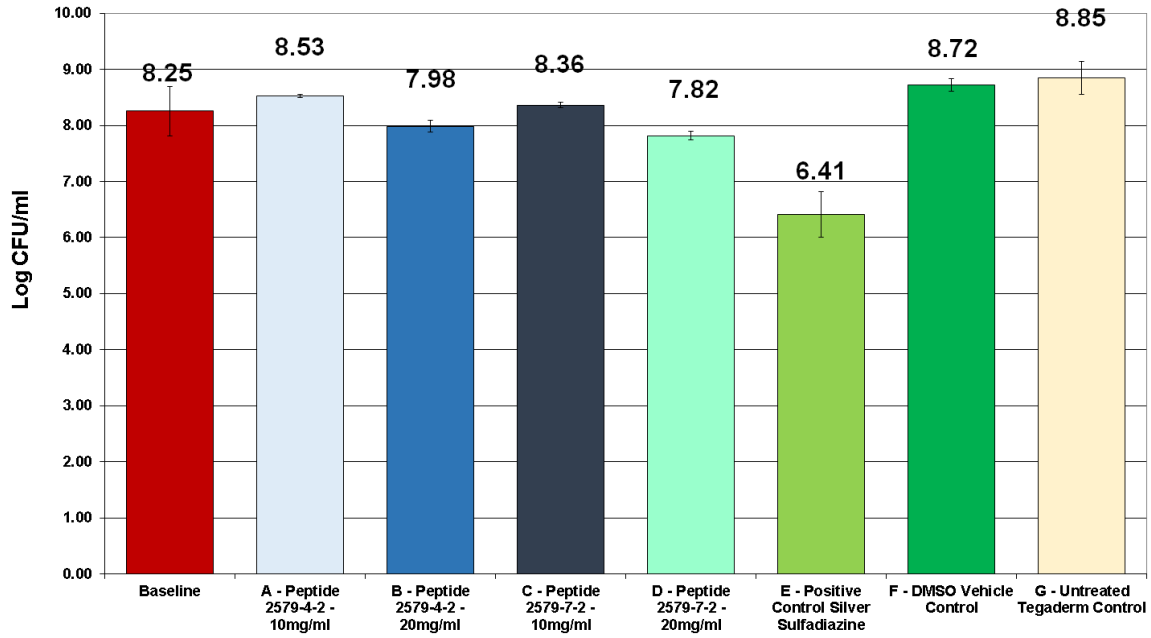

David Devore (Rutgers) who was a subcontract on partnering Torrey Pines grant optimized the cyclic lipopeptide/graft copolymer nanocomplexes formulations to test *in vivo*.

We created forty-eight partial thickness wounds (10x7x0.5mm) on the back with an electrokeratome. Wounds were inoculated with 25 µl of the suspension 10^6 MRSA suspension that was scrubbed into each wound. Eight wounds were assigned to one of the following treatment groups: A) nanoformulation + peptide 2579-7 (1.7mg/ml), B) nanoformulation vehicle, C) DMSO + peptide 2579-7 (1.7mg/ml), D) DMSO vehicle, E) Mupirocin positive control and F) untreated control. All treatments including untreated were covered with a polyurethane film dressing to prevent possible cross contamination. Wounds were treated daily and four wounds from each treatment group were recovered from each treatment group on days 2 and 5 post treatment as described previously.

Figure 12: MRSA counts after nano-formulation treatment

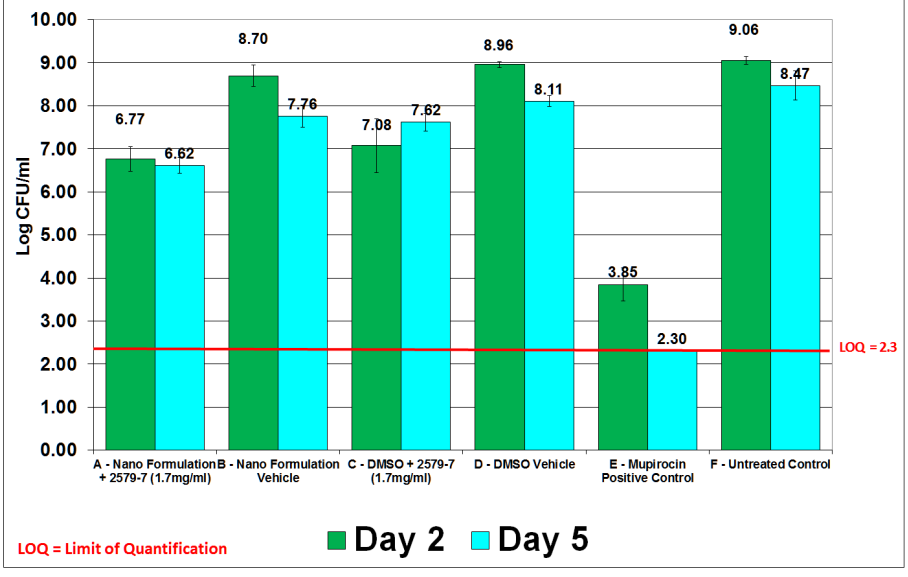

As seen from the data (**Figure 12**) on Day 2 the nanofomulation with peptide was able to reduce the MRSA counts by 2 and 2.3 log CFU/ml as compared nanoformulation vehicle and untreated control respectively. The Nanofomulation

with peptide was also able to reduce the MRSA counts by 0.3 log CFU/ml and 1 log CFU/ml on days 2 and 5 respectively as compared to DMSO + peptide thus showing an additional benefit of the delivery system. We did see that our positive control mupirocin showed the hightest reduction in MRSA counts with 3.85 and 2.3 log CFU/ml on days 2 and 5 respectively.

Dr. Davore was able to optimize the formulation with a higher peptide concentration (7mg/ml). As compared to the previous animal with the same peptide at a lower concentration (1.7mg/ml – see **Figure 12**), the higher concentration (7mg/ml) was over 2 log CFU/ml more effective when formulated in the nanoformulation. As seen in **Figure 13** topical mupirocin was again the most effective treatment against MRSA followed by Nanoformulation + 2579-7 and Nanoformulation + 2579-4, respectively. Nanoformulation 2579-7 was found to be statistically more effective than Nanoformlation + 2579-4 on day 1. Both of the nanopeptide peptide formulations were found to have enhanced antimicrobial activity as compared DMSO delivery. The untreated control wounds and vehicles (nanoformulation and DMSO) had the highest MRSA counts (Days 1 and 5).

Figure 13: MRSA counts after nano-formulation treatment (7mg/ml)

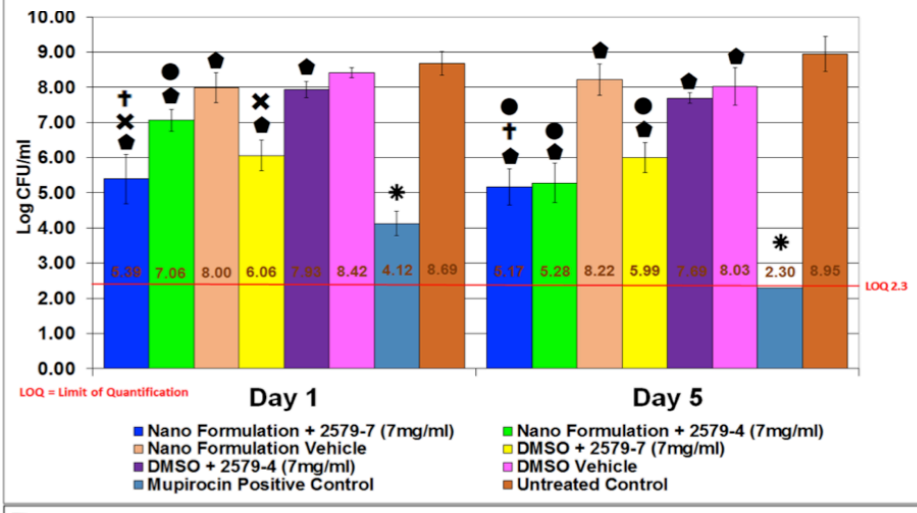

Day 1
*p<0.05 compared to all treatments †p<0.05 compared to DMSO + 2579-7 (7mg/ml) •p<0.05 compared to Untreated Control
×p<0.05 compared to Nano Formulation + 2579-4 (7mg/ml), Nano Formulation Vehicle, DMSO + 2579-4 (7mg/ml) and DMSO Vehicle
•p<0.05 compared to Nano Formulation Vehicle, DMSO + 2579-4 (7mg/ml) and DMSO Vehicle

Day 5
*p<0.05 compared to all treatments †p<0.05 compared to DMSO + 2579-7 (7mg/ml) •p<0.05 compared to Untreated Control
•p<0.05 compared to Nano Formulation Vehicle, DMSO + 2579-4 (7mg/ml) and DMSO Vehicle

After these studies, Torrey Pines completed additional *in vitro* analysis of new peptides (See Partnering PI report) and found that 4 had higher antimicrobial activity as compared to previously examined peptides. Since Dr. Davore told Torrey Pines that he has run out of funding to work on more nanoformulations, we decided to perform a pilot study using the 4 most active peptides (at various concentrations) in DMSO against biofilm bacteria (treated after 24 hours of inoculation). We used our porcine full thickness wound model against a military isolate of *Pseudmonas aurginosa* (PA-09-10).

Briefly, forty eight (48) full thickness wounds were made on the paravertebral and thoracic area with an 8mm punch biopsy. Wounds were inoculated with 10^6 log CFU/ml and covered for 24 hours to allow for biofilm formation. Three (3) wounds were assigned to each treatment group and three wounds were used as baseline (recovered after 24 hour biofilm formation and prior to treatment).

Four (4) wounds were biopsied 10mm punch biopsy per group per animal, on days 2 and 5 post treatment application. The punch biopsy was taken around entire wound and removed down to subcutaneous tissue in order to evaluate bacteria on wound edges, bed and surface. Biopsies were weighed then immediately placed in 1 ml of All Purpose Neutralizing Solution. The sample was combined with an additional 4 ml of Neutralizing Solution and homogenized in a sterile homogenization tube (Tenbroeck Tissue Grinder). Serial dilutions were made and scrub solutions were quantified using the Spiral Plater System. ORSAB media was used to isolate MRSA from the wounds. After plating, all samples were incubated aerobically for 24 hours at 37° C. After the incubation period, colonies on the plates were counted and the CFU/g calculated. The data were combined and analyzed for significant differences between treatments using One-way ANOVA analysis.

All peptides showed a dose response effect against PA (**Figure 14** below). The lowest PA counts were found in wounds that were treated with peptide 2612-8.1 at 20 mg/ml (6.18 log CFU/g). This was followed by positive control (silver sulfadiazine) which had 6.32 log CFU/g. The next most effective peptide was peptide 2612-8.2 (20 mg/ml) which had PA counts of 6.45 log CFU/g. The highest concentration (20 mg/ml) of peptides 2612-16 and 2612-13 had similar PA counts with 6.84 log CFU/g and 6.86 log CFU/g, respectively. The untreated control and DMSO treated wounds had the highest PA counts with 8.65 log CFU/g and 8.42 log CFU/g, respectively. The most effective peptide (2612-8.1) was 2.47 log CFU/g lower than untreated control and 2.24 log CFU/g lower than DMSO vehicle control.

Figure 14: Bacterial counts of P. aeruginosa PA09-010 after treatment application

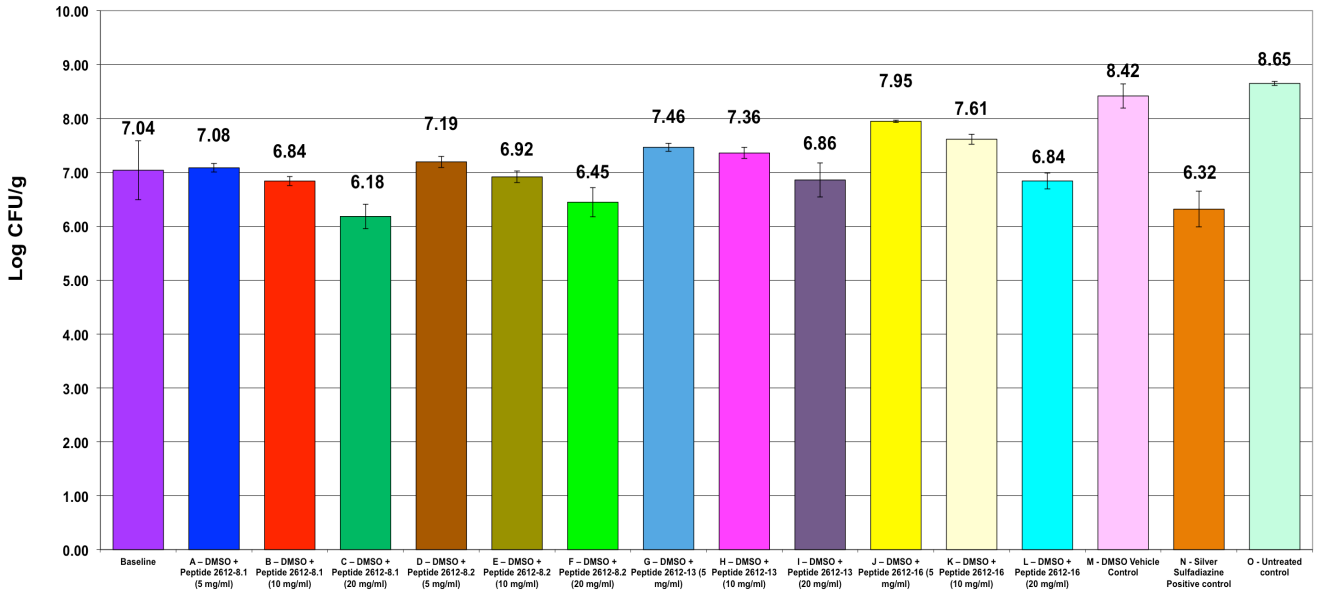

Using the most effective peptide (2612-8.1), we performed additional animals for statistics. The treatment group with the lowest bacterial count on day 2 (5.25±0.28 Log CFU/g) was DMSO + Peptide 2612-8.1 (20 mg/ml) as shown in Figure 6. This resulted in bacterial reductions of at least 99.30% when compared against both baseline wounds and those wounds left untreated. Wounds treated with Silver Sulfadiazine (positive control) showed a count of 5.70±0.32 Log CFU/g which was lower than DMSO vehicle and untreated control (**Figure 15**).

On day 5 wounds treated with DMSO + Peptide 2612-8.1 (20 mg/ml) again exhibited the PA counts (4.62±0.40 Log CFU/g). This bacterial count resulted in the largest bacterial difference when compared against Untreated control (3.82±0.13 Log CFU/g), which yields a bacterial reduction of 99.98%. Treatment with DMSO + Peptide 2612-8.1 (20 mg/ml) showed significantly ($p < 0.05$) lower PA counts than all other treatment groups in this study including Silver Sulfadiazine.

Figure 15: Bacterial counts of *P. aeruginosa* PA09-010 after treatment application

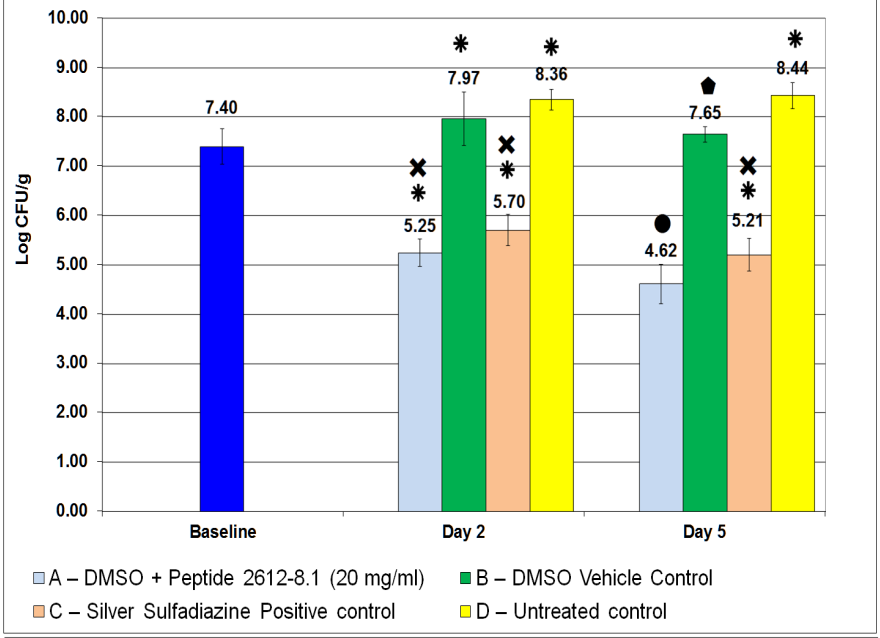

Torrey Pines performed additional *in vitro* assessments and found that peptide 2605-4 had greater activity as compared with the previous peptides we examined. We then

used our porcine full thickness wound model to evaluate its effects against Methicillin Resistant Staphylococcus aureus (MRSA) USA300 biofilms. Briefly, forty eight (48) full thickness wounds were created on the paravertebral and thoracic area of two pigs with an 8mm punch biopsy. Wounds were inoculated with 10^6 log CFU/ml and covered for 24 hours to allow for biofilm formation. After biofilm formation, wounds were treated daily with enough material to completely cover the wound and normal surrounding skin. Treatments included: 1) Peptide 2605-4 [20 mg/ml] dissolved in DMSO, 2) DMSO vehicle alone, 3) Mupirocin - positive control, and 4) Untreated control. Wounds were randomly divided into four (4) groups of 8 wounds each with four wounds were used for baseline counts (to determine counts prior to treatment).

The baseline wounds had a MRSA count of 7.75 Log CFU/g (**Figure 16**). On day 2, Untreated control and DMSO Vehicle Control had the highest MRSA counts (8.21 and 7.38 Log CFU/g, respectively). Wounds treated with Mupirocin Positive control and DMSO = Peptide 2605-2 (20 mg/ml) had the lowest MRSA counts of 3.94 and 4.84 Log CFU/g, respectively. Both of these treatments groups demonstrated significantly lower MRSA counts than DMSO vehicle, untreated control, and baseline (both day 2 and 5 post treatment). Mupirocin treated wounds showed significantly lower MRSA values as compared to DMSO + Peptide 2605-4 (both assessment days).

Figure 16: MRSA Counts

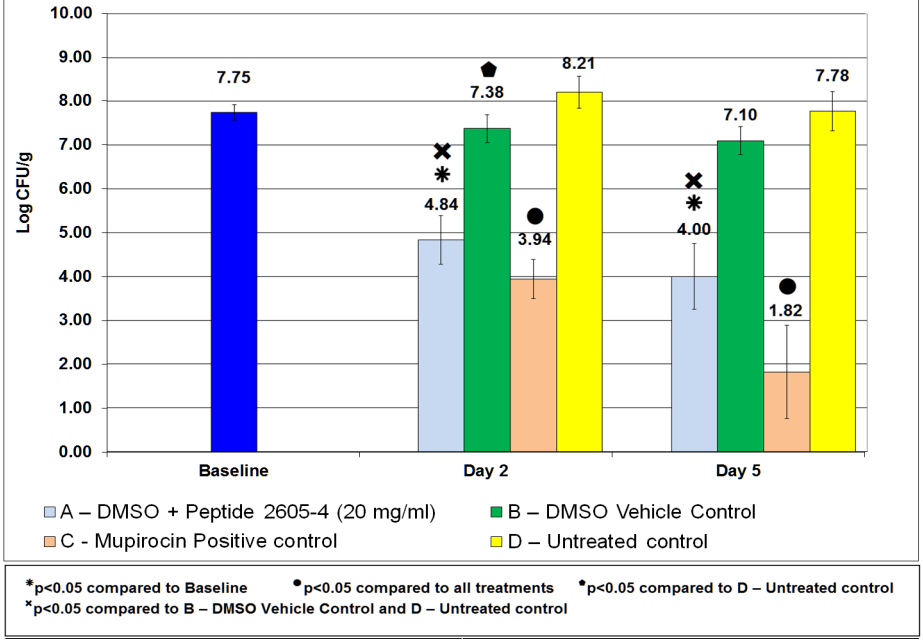

Based on CFU determination and observed reduction of MRSA load observed on day 5 we analyzed expression of the MRSA virulence in wounds treated with 2605-4 incorporated dissolved in DMSO. Total RNA was extracted from total of forty wounds at baseline and post-treatment from all infected and treated wounds as well as untreated control samples. cDNA was generated with Reverse transcription and DNase treatment using Quantitect Reverse Transcription Kit (Qiagen) followed by qPCR (IQ Supermix, Quanta). Gene expression quantification was performed in triplicates using the CFX96 real-time PCR system (Bio-Rad). A mock reaction without addition of reverse transcriptase was used to ensure that amplification was specific for mRNA, while DNA was completely eliminated. We determined relative expression of the MRSA virulence factors staphylococcal protein A (spA), Panton-Valentine leukocidin (pvl), and α-hemolysin (hla).

SpA is known for its role in modulation of the host immune system. SpA inhibits the mechanisms of host adaptive immunity by binding host antibody molecules in the Fc region, which is the opposite direction foreign particles are usually bound. This allows Staphylococcus to trick mammalian immune system by recognizing the bacterial cell as one of its own cells.
Another pathogenic property of SpA is its ability to bind to and activate the TNFα receptor, which leads to prolonged inflammation. Gene expression analyses have shown that treatment with 2605-4 resulted in suppression of spA compared to levels detected in wounds prior to treatment (baseline), or control

untreated wounds and wounds treated with vehicle –DMSO (**Figure 17**). No significant suppression of spA was observed compared to mupirocin treated wounds. In summary peptide 2605-4 has shown ability to suppress MRSA virulence through modulation of SpA, thus further enhancing elimination of this pathogen. Specific formulation allowing sustained delivery of 2605-4 or increased concentration of peptide may result in even more efficient antimicrobial effect and further reduction of pathogen's virulence.

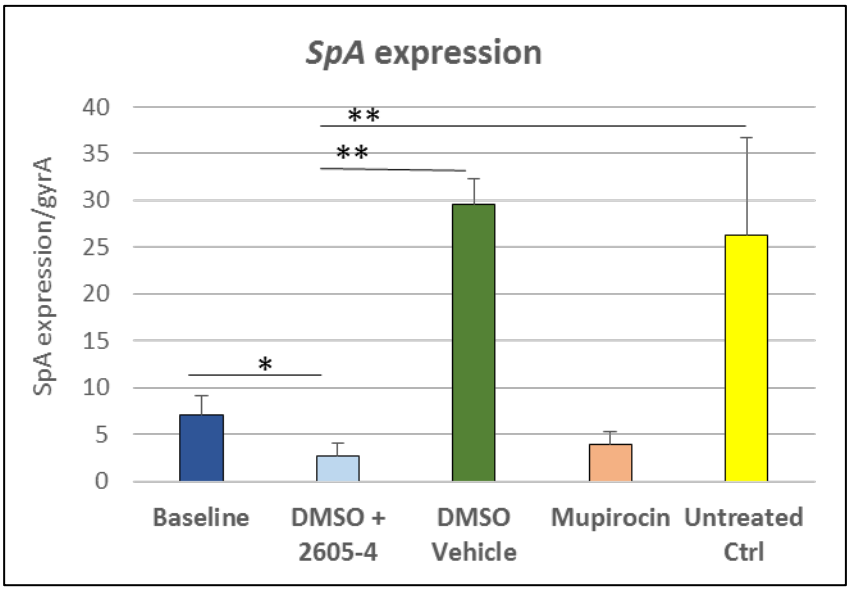

Figure 17. RT-PCR results for *spA* expression in wounds infected with MRSA USA300 and treated with peptide 2605-4 in DMSO. The relative expression levels were normalized to gyrA. Error bars indicate SEM. *statistically significant differences defined as p<0.05; ** p<0.01

Alpha-hemolysin, also known as alpha-toxin, is the major cytotoxic agent released by S. aureus and the first identified member of the pore forming beta-barrel toxin family. The hla protein monomer forms heptameric units on the cellular membrane to form complete beta-barrel pore. This structure allows the toxin to perform its major function, development of pores in the cellular membrane, eventually causing cell death. Hla also plays a role in S. aureus invasion through human epidermal keratinocytes. Gene expression analyses for hla has shown suppression of this virulence factor in wounds treated with peptide 2605-4 dissolved in vehicle compared to mupirocin treated wounds (**Figure 18**). Low levels of hla expression were found in wounds treated with peptide 2605-4, DMSO and also control wounds compared to baseline and mupirocin treated wounds.

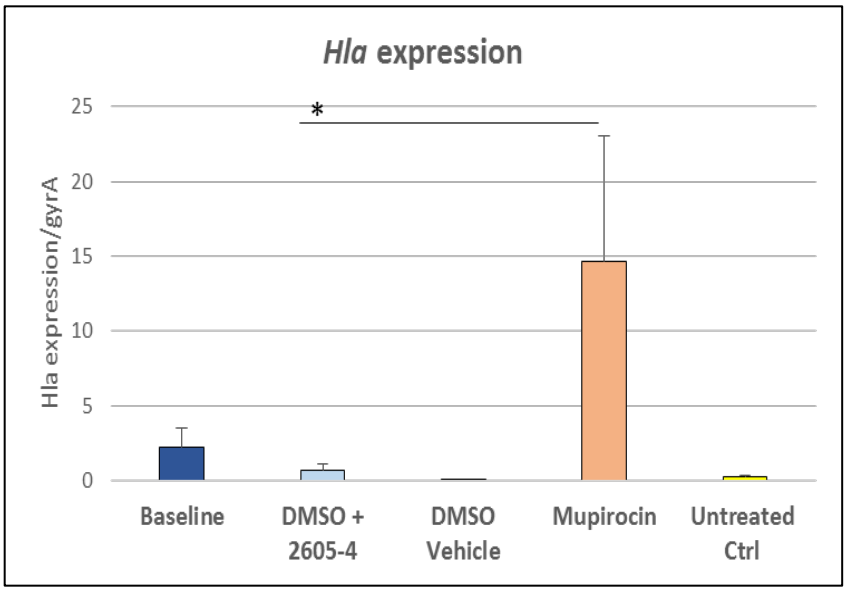

Figure 18. RT-PCR results for *Hla* expression in wounds infected with MRSA USA300 and treated with peptide 2605-4. The relative expression levels were normalized to gyrA. Error bars indicate SEM. *statistically significant differences were defined as p<0.05.

We also evaluated expression levels of Pvl the pore forming virulence factor which primarily targets neutrophils therefore affecting host immune response. Gene expression analyses have not found significant differences in Pvl levels between baseline, 2605-4 treated wounds and untreated control (**Figure 19**). Significant variation within the treatment group may be a result of variability in extent of

healing. Further evaluation of host response and extent of wound healing will be correlated with the gene expression of MRSA virulence factors.

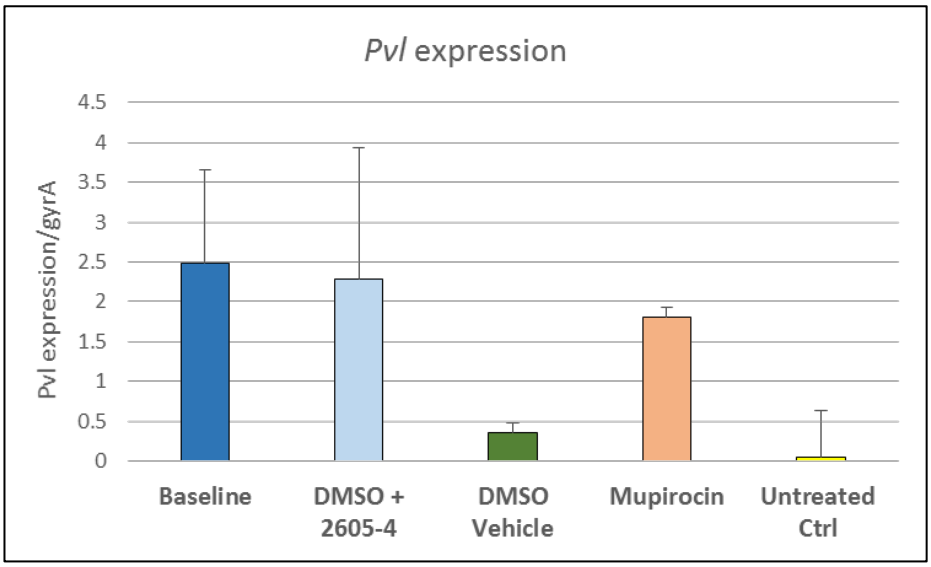

Figure 19. RT-PCR results for pvl expression in wounds infected with MRSA USA300 and treated with peptide 2605-4. The relative expression levels were normalized to gyrA. Error bars indicate SEM.

Major Task 9: Effects of lipopeptide formulations on wound healing.
Subtask 1: Assess effects of selected lipopeptides and lipopeptide/polymer nanocomplexes on wound healing.
Materials and Methods
Forty-eight (48) full thickness wounds were made on the paravertebral and thoracic area with an 8mm punch biopsy. Treatment groups (4) were randomly assigned to different anatomical areas on each pig. Twelve (12) wounds were assigned to each treatment group.

Treatment Regimen
Within 20 minutes after wounding all wounds were treated daily with 100 ul to cover the wounded area and surrounding unwounded skin. After treatment application wounds were covered with a polyurethane film dressing (Tegaderm; 3M, St. Paul, MN). Untreated control wounds received polyurethane film alone.

Histological Assessment
A total of eight biopsies were taken from each treatment group on days 5, 7 and 10 after wounding. Incisional biopsies were obtained through the center of the wounds including normal adjacent skin on both sides. Each tissue sample was placed in formalin then stained with hematoxylin and eosin (H&E). One section per block was analyzed.

Each tissue sample was evaluated semi-quantitatively and blindly by a dermato-pathologist via light microscopy and examined for the following elements to determine a potential local tissue response to the test formulations.
The histological analysis was performed blindly without knowing the treatment for each group. Combining the data from each animal a total of eight tissue specimens from each treatment group at each time point were analyzed for statistical analysis.

Results

Percentage of re-epithelialization

The percent of re-epithelialization represents the percent of the wound area covered by newly formed epidermis with one or more layers of keratinocytes, which is a good index for the speed of keratinocyte migration and the first step of the re-epithelialization.

On day 5, wounds treated with DMSO (vehicle) exhibited a significantly ($p < 0.05$) higher percentage re-epithelialized (75.7%) when compared against wounds treated with Peptide 2605-4 (20mg/ml) (43.8% - see **Figure 20** below). On day 7, those wounds left untreated showed the highest amount of re-epithelialization at 96.0%. While Peptide 2612-8.1 (20mg/ml) had 85.9% of epithelialization. Both Untreated Tegaderm Control and Peptide 2612-8.1 (20mg/ml) showed significantly ($p < 0.05$) higher results than Peptide 2605-4 (20mg/ml). By day 10, all wounds were past the 90% threshold, except those wounds treated with Peptide 2605-4 (20mg/ml) at 72.2% (significantly lower than all other groups). Both wounds treated with Peptide 2612-8.1 (20mg/ml) and DMSO (vehicle) reached at least 95.4%, while those wounds left untreated were fully re-epithelialized by the end of the study.

Figure 20: % Epithelialization

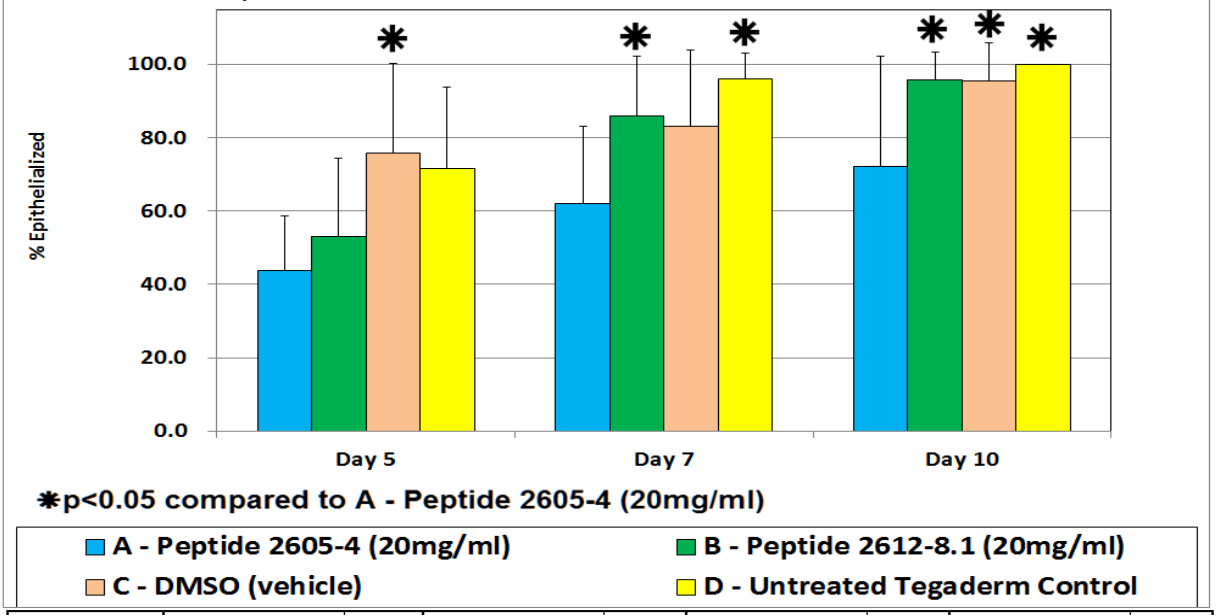

%Epithelialized	A - Peptide 2605-4 (20mg/ml)	Std dev	B - Peptide 2612-8.1 (20mg/ml)	Std dev	C - DMSO (vehicle)	Std dev	D - Untreated Tegaderm Control	Std dev
Day 5	43.8	15.034	53.0	21.449	75.7	24.683	71.7	22.207
Day 7	62.0	21.020	85.9	16.300	83.0	20.904	96.0	7.068
Day 10	72.2	29.938	95.9	7.571	95.4	10.542	100.0	0.000

DAY=5

* p<0.05 statistical significance

Treatment	A - Peptide 2605-4 (20mg/ml)	B - Peptide 2612-8.1 (20mg/ml)	C - DMSO (vehicle)	D - Untreated Tegaderm Control
A - Peptide 2605-4 (20mg/ml)		0.819	**0.026***	0.061
B - Peptide 2612-8.1 (20mg/ml)	0.819		0.164	0.310
C - DMSO (vehicle)	**0.026***	0.164		0.981
D - Untreated Tegaderm Control	0.061	0.310	0.981	

DAY=7

* p<0.05 statistical significance

Treatment	A - Peptide 2605-4 (20mg/ml)	B - Peptide 2612-8.1 (20mg/ml)	C - DMSO (vehicle)	D - Untreated Tegaderm Control
A - Peptide 2605-4 (20mg/ml)		**0.046***	0.094	**0.003***
B - Peptide 2612-8.1 (20mg/ml)	**0.046***		0.987	0.649
C - DMSO (vehicle)	0.094	0.987		0.447
D - Untreated Tegaderm Control	**0.003***	0.649	0.447	

DAY=10

* p<0.05 statistical significance

Treatment	A - Peptide 2605-4 (20mg/ml)	B - Peptide 2612-8.1 (20mg/ml)	C - DMSO (vehicle)	D - Untreated Tegaderm Control
A - Peptide 2605-4 (20mg/ml)		**0.034***	**0.039***	**0.010***
B - Peptide 2612-8.1 (20mg/ml)	**0.034***		1.000	0.958
C - DMSO (vehicle)	**0.039***	1.000		0.941
D - Untreated Tegaderm Control	**0.010***	0.958	0.941	

Epithelial thickness

The epithelial thickness was a measure of an average thickness of five points of newly formed epithelium. Epithelial thickness reflects the process of keratinocyte proliferation, differentiation and epidermal maturation.

On day 5, all treatment groups showed similar measurements when compared against each other, with results ranging from 117.9 to 124.8 µm (**Figure 21**). By day 7, all wounds had a slightly bigger measurement with both Peptide 2650-4 (20mg/ml) and Peptide 2612-8.1 (20mg/ml) having thicker measurements at 137.7 µm. On day 10, the only group showing a lower epithelial thickness were those left untreated at 125.7 µm. While those wounds treated with Peptide 2612-8.1 (20mg/ml) exhibited the highest epithelial thickness measurements among all wounds for the entire study (140.7 µm). Despite DMSO (vehicle) having a slight increment on day 10 (133.5 µm), both of the Peptide treatment groups remained slightly bigger by the end of the study. There were no statistical significant differences when making comparisons among treatment groups on any of the time points.

Figure 21: Epithelial Thickness

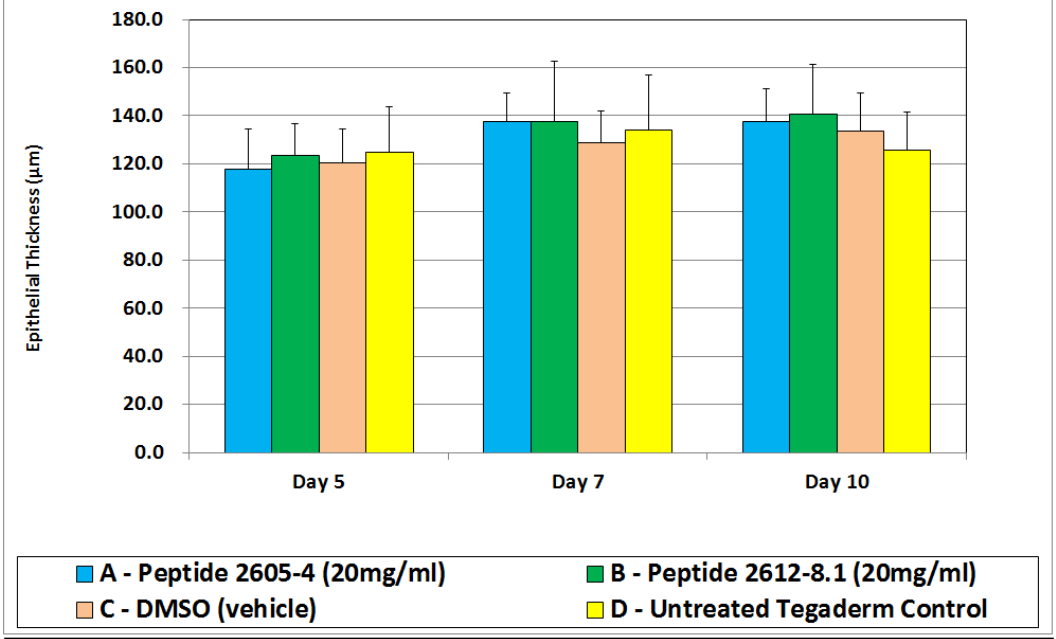

Epithelial Thickness	A - Peptide 2605-4 (20mg/ml)	Std dev	B - Peptide 2612-8.1 (20mg/ml)	Std dev	C - DMSO (vehicle)	Std dev	D - Untreated Tegaderm Control	Std dev
Day 5	117.9	16.748	123.3	13.573	120.3	14.079	124.8	19.028
Day 7	137.7	11.612	137.7	25.104	128.7	13.451	134.1	22.712
Day 10	137.7	13.512	140.7	20.563	133.5	15.865	125.7	15.813

DAY=5

* p<0.05 statistical significance

Treatment	A - Peptide 2605-4 (20mg/ml)	B - Peptide 2612-8.1 (20mg/ml)	C - DMSO (vehicle)	D - Untreated Tegaderm Control
A - Peptide 2605-4 (20mg/ml)		0.906	0.990	0.824
B - Peptide 2612-8.1 (20mg/ml)	0.906		0.982	0.998
C - DMSO (vehicle)	0.990	0.982		0.942
D - Untreated Tegaderm Control	0.824	0.998	0.942	

DAY=7

* p<0.05 statistical significance

Treatment	A - Peptide 2605-4 (20mg/ml)	B - Peptide 2612-8.1 (20mg/ml)	C - DMSO (vehicle)	D - Untreated Tegaderm Control
A - Peptide 2605-4 (20mg/ml)		1.000	0.783	0.981
B - Peptide 2612-8.1 (20mg/ml)	1.000		0.783	0.981
C - DMSO (vehicle)	0.783	0.783		0.942
D - Untreated Tegaderm Control	0.981	0.981	0.942	

DAY=10

* p<0.05 statistical significance

Treatment	A - Peptide 2605-4 (20mg/ml)	B - Peptide 2612-8.1 (20mg/ml)	C - DMSO (vehicle)	D - Untreated Tegaderm Control
A - Peptide 2605-4 (20mg/ml)		0.984	0.957	0.484
B - Peptide 2612-8.1 (20mg/ml)	0.984		0.822	0.293
C - DMSO (vehicle)	0.957	0.822		0.785
D - Untreated Tegaderm Control	0.484	0.293	0.785	

White cell infiltration

White cell infiltration (WCI) is used to access the inflammation reaction that could be a normal process of wound repair or due to microbial infection or the tissue reaction to foreign materials in the wound.
All treatments groups showed white cell infiltration scores ranging from 4.2 to 4.5 (**Figure 22**). Hence, there were no statistical significant differences when comparing among treatment groups. While only those wounds treated with Peptide 2605-4- (20mg/ml) showed the highest score (4.5) for the entire study.

Figure 22: White Cell Infiltrate

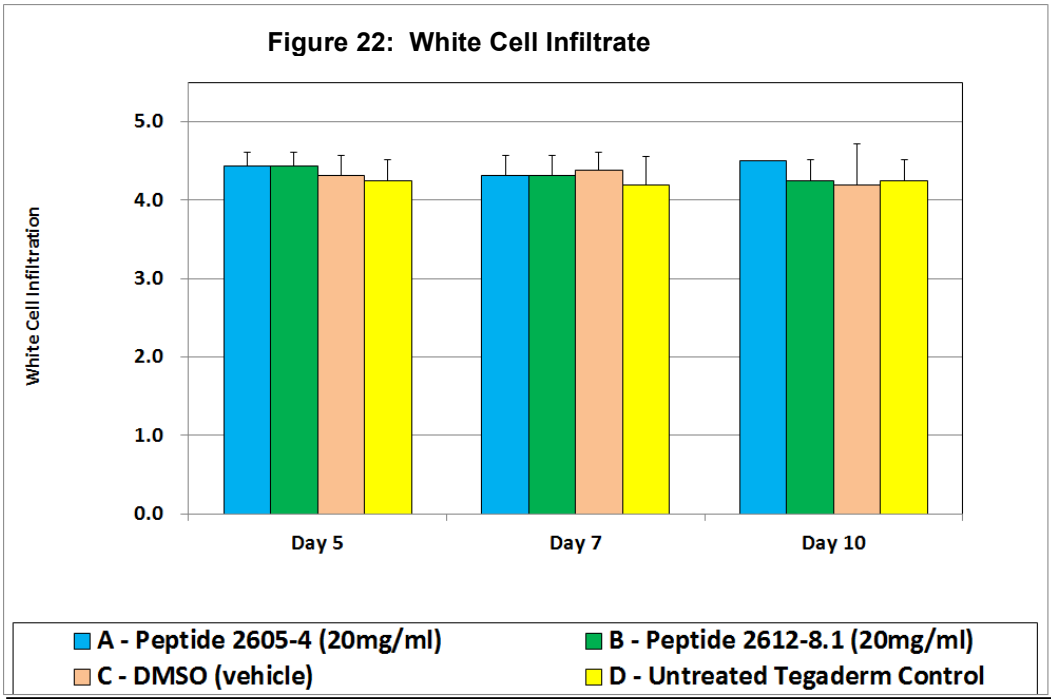

White Cell Infiltration	A - Peptide 2605-4 (20mg/ml)	Std dev	B - Peptide 2612-8.1 (20mg/ml)	Std dev	C - DMSO (vehicle)	Std dev	D - Untreated Tegaderm Control	Std dev
Day 5	4.4	0.177	4.4	0.177	4.3	0.259	4.3	0.267
Day 7	4.3	0.259	4.3	0.259	4.4	0.231	4.2	0.372
Day 10	4.5	0.000	4.3	0.267	4.2	0.530	4.3	0.267

DAY=5

*** p<0.05 statistical significance**

Treatment	A - Peptide 2605-4 (20mg/ml)	B - Peptide 2612-8.1 (20mg/ml)	C - DMSO (vehicle)	D - Untreated Tegaderm Control
A - Peptide 2605-4 (20mg/ml)		1.000	0.683	0.356
B - Peptide 2612-8.1 (20mg/ml)	1.000		0.683	0.356
C - DMSO (vehicle)	0.683	0.683		0.944
D - Untreated Tegaderm Control	0.356	0.356	0.944	

DAY=7

*** p<0.05 statistical significance**

Treatment	A - Peptide 2605-4 (20mg/ml)	B - Peptide 2612-8.1 (20mg/ml)	C - DMSO (vehicle)	D - Untreated Tegaderm Control
A - Peptide 2605-4 (20mg/ml)		1.000	0.971	0.817
B - Peptide 2612-8.1 (20mg/ml)	1.000		0.971	0.817
C - DMSO (vehicle)	0.971	0.971		0.562
D - Untreated Tegaderm Control	0.817	0.817	0.562	

DAY=10

*** p<0.05 statistical significance**

Treatment	A - Peptide 2605-4 (20mg/ml)	B - Peptide 2612-8.1 (20mg/ml)	C - DMSO (vehicle)	D - Untreated Tegaderm Control
A - Peptide 2605-4 (20mg/ml)		0.431	0.243	0.431
B - Peptide 2612-8.1 (20mg/ml)	0.431		0.980	1.000
C - DMSO (vehicle)	0.243	0.980		0.980
D - Untreated Tegaderm Control	0.431	1.000	0.980	

Granulation tissue formation

The dermal reconstitution begins in about 3 to 4 days of injury with the hallmark of granulation tissue formation, which include new blood vessel formation (angiogenesis), and the accumulation of fibroblasts and collagen extracellular matrices. The granulation tissue formation measures the percent of wound bed filled with newly formed granulation tissue.

On day 5, both Peptide treated wounds were significantly ($p < 0.05$) lower than DMSO (vehicle) and Untreated Tegaderm Control by almost half of the score (**Figure 23**). This difference diminished by day 7 since all wounds reached granulation tissue formation scores higher than 3. Untreated
Tegaderm Control showed a significantly ($p < 0.05$) higher score than Peptide 2605-4(20mg/ml). On day 10, all wounds reached scores higher than 4, with those wounds left untreated continuing to have the highest score while having significantly ($p < 0.05$) higher score than Peptide 2605-4(20mg/ml).

Figure 23: Granulation Tissue Formation

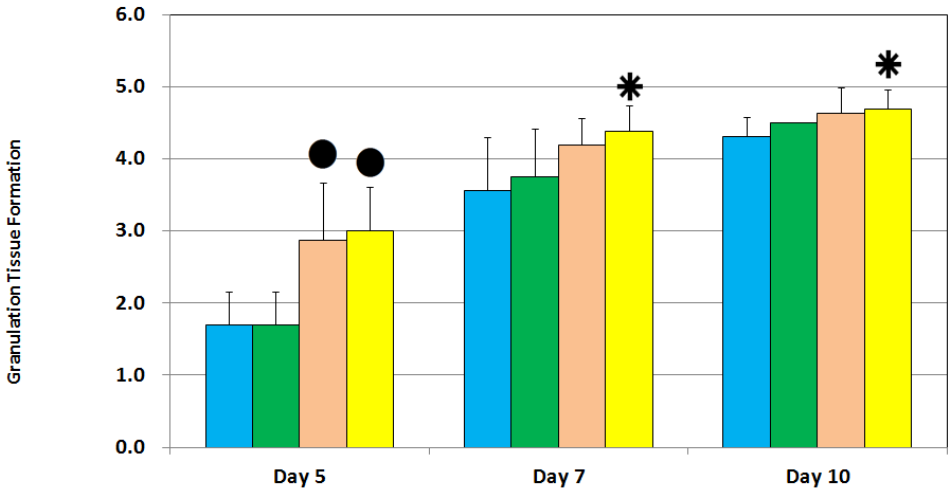

Granulation Tissue	A - Peptide 2605-4 (20mg/ml)	Std dev	B - Peptide 2612-8.1 (20mg/ml)	Std dev	C - DMSO (vehicle)	Std dev	D - Untreated Tegaderm Control	Std dev
Day 5	1.7	0.458	1.7	0.458	2.9	0.791	3.0	0.598
Day 7	3.6	0.729	3.8	0.655	4.2	0.372	4.4	0.354
Day 10	4.3	0.259	4.5	0.000	4.6	0.354	4.7	0.259

DAY=5

* p<0.05 statistical significance

Treatment	A - Peptide 2605-4 (20mg/ml)	B - Peptide 2612-8.1 (20mg/ml)	C - DMSO (vehicle)	D - Untreated Tegaderm Control
A - Peptide 2605-4 (20mg/ml)		1.000	**0.002***	**0.001***
B - Peptide 2612-8.1 (20mg/ml)	1.000		**0.002***	**0.001***
C - DMSO (vehicle)	**0.002***	**0.002***		0.974
D - Untreated Tegaderm Control	**0.001***	**0.001***	0.974	

DAY=7

* p<0.05 statistical significance

Treatment	A - Peptide 2605-4 (20mg/ml)	B - Peptide 2612-8.1 (20mg/ml)	C - DMSO (vehicle)	D - Untreated Tegaderm Control
A - Peptide 2605-4 (20mg/ml)		0.905	0.132	**0.031***
B - Peptide 2612-8.1 (20mg/ml)	0.905		0.405	0.132
C - DMSO (vehicle)	0.132	0.405		0.905
D - Untreated Tegaderm Control	**0.031***	0.132	0.905	

DAY=10

* p<0.05 statistical significance

Treatment	A - Peptide 2605-4 (20mg/ml)	B - Peptide 2612-8.1 (20mg/ml)	C - DMSO (vehicle)	D - Untreated Tegaderm Control
A - Peptide 2605-4 (20mg/ml)		0.466	0.089	**0.031***
B - Peptide 2612-8.1 (20mg/ml)	0.466		0.760	0.466
C - DMSO (vehicle)	0.089	0.760		0.960
D - Untreated Tegaderm Control	**0.031***	0.466	0.960	

In summary both peptides (2605-4 and 2612-8.1) delayed epithelialization and decreased granulation tissue formation on day 5 post wounding. Peptide 2605-4 continued to show inhibitory effects on epithelialization throughout the study. We are currently analyzing data from another animal and will combine data for statistics to substantiate these findings.

Molecular Assessment

Additional biopsies (4mm) were taken from the two treated animals on days 5, 7 and 10 for the molecular analyses of host response. The biopsies were immediately submerged in RNAlater and stored at 4oC overnight for stabilization. RNA was isolated using Direct-zol RNA Mini Kit (Zymo Research) following manufacturer's instructions. Samples were assessed for expression levels of genes important for wound healing and inflammation interleukin-1 (IL-1α), interleukin-8 (IL-8), and tumor necrosis factor α (TNFα). For real-time qPCR, 10 ng of total RNA from porcine skin

wound tissue was reverse transcribed and amplified using One-Step RT-PCR Kit (Quanta). Real-time PCR was performed in triplicates using the CFX96 real-time PCR system (Bio-Rad). Relative expression was normalized to levels of GAPDH. The primer sequences used were: GAPDH, forward (5′-ACATCATCCCTGCTTCTAC-3′) and reverse (5′-TTGCTTCACCACCTTCTTG-3′); IL-1α, forward (5′-GCCAATGACACAGAAGAAG-3′) and reverse (5′-TCCAGGTTATTTAGCACAGC-3′); IL-8, forward (5′-GACCAGAGCCAGGAAGAGAC-3′) and reverse (5′-GGTGGAAAGGTGTGGAATGC-3′); TNFα forward (5′- CACGCTCTTCTGCCTACTG -3′) and reverse (5′-ACGATGATCTGAGTCCTTGG -3′). Comparison of gene expression data for each treatment group was performed using GraphPad. The means were analyzed by t test and significance was defined as a $p<0.01$.

Molecular Analysis

IL-1α Expression

IL-1α is an important mediator of the inflammatory response. During cutaneous wound healing IL-1α is expressed initially by keratinocytes followed by predominant expression from infiltrating neutrophils. IL-1α promotes neutrophil recruitment from the circulation to the wound site during early inflammatory phase, which is required for bacterial clearance. Proliferative phase of wound healing is marked by suppression of this pro-inflammatory cytokine.

On day 5 and 7 post-treatment, wounds from all conditions have shown comparable expression levels of IL-1α corresponding to inflammatory phase of the wound healing process (**Figure 24**). However on day 10 wounds treated with the peptide 2605-4 (group A) have shown high level of IL-1α while the expression levels of this pro-inflammatory molecule has ceased in all other treatment conditions. This data suggest that wounds treated with 2605-4 were not shifting from inflammatory to proliferative phase of wound healing, contributing to delayed wound closure as observed by histopathology analyses. Treatment with the peptide 2612-8.1 resulted in suppression of IL-1α at day 10 comparable to levels observed in vehicle (DMSO) and control untreated wounds thus corresponding to observed healing in wounds treated with this peptide.

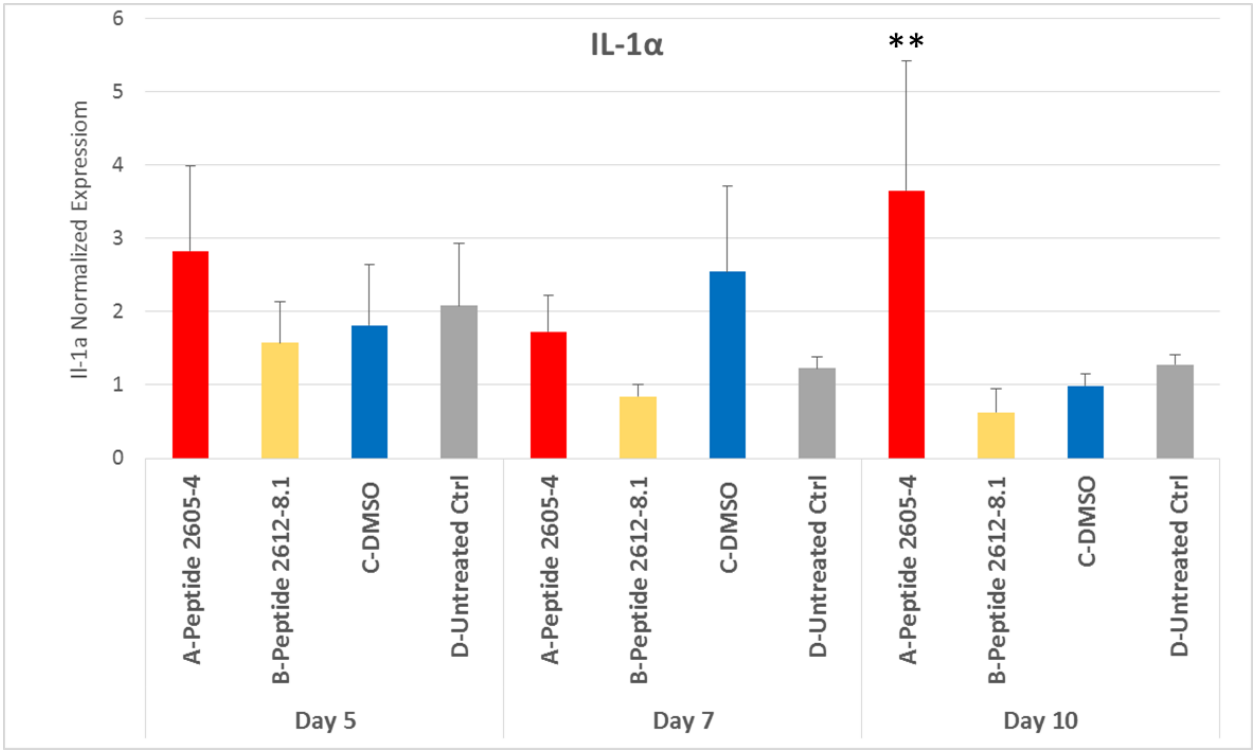

Figure 24. Treatment with the 2605-4 resulted in marked induction of IL-1α at day 10. Mean values of expression levels were represented after normalization to GAPDH (n=4). Error bars indicate SEM. **statistically significant differences were defined as $p<0.01$ compared to vehicle treated wounds.

IL-8 Expression

Interleukin 8 (IL-8) is a neutrophil chemo-attractants produced early in the inflammatory phase of wound healing. Once at the wound area neutrophils continue production of neutrophil chemo-attractants including IL-8 to replenish their numbers as cells die during the bacterial clearance. Expression of IL-8 is the highest in initial inflammatory phases of wound healing, while suppression of this pro-inflammatory cytokine is required for proliferative phase and wound closure. At day 5 wounds treated with the peptide 2605-4 had the highest expression of IL-8 compared to all treatment groups (**Figure 25**). While IL-8 expression was overall lower at day 7, striking induction of this pro-inflammatory cytokine occurred at day 10 in wounds treated with 2605-4 and 2612-8.1, with a more robust levels of IL-8 in wounds treated with the peptide 2605-4 . The observed induction of IL-8 may also contribute to delay healing and prolonged inflammation observed in wounds treated with 2605-4, and also lower score for granulation tissue formation observed in wounds treated with 2605-4 and 2612-8.1

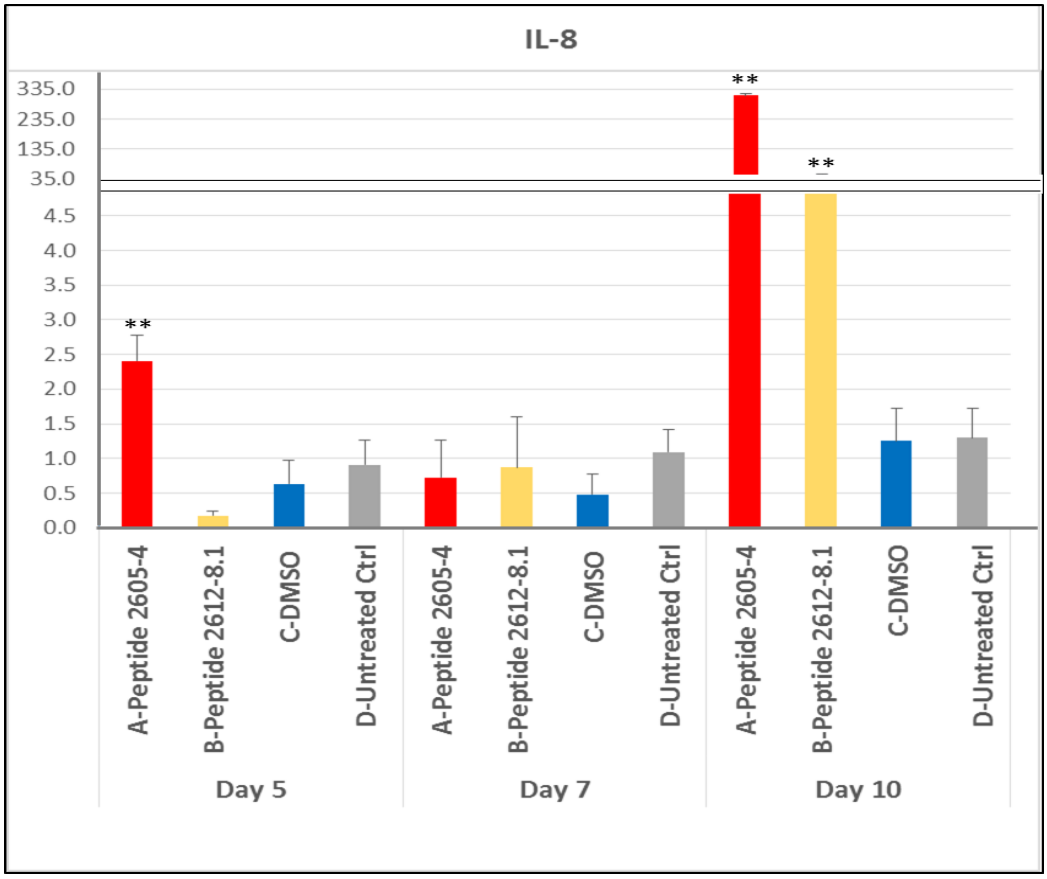

Figure 25. 2605-4 and 2612-8.1 treatments resulted in induced expression of IL-8. Mean values of expression levels were represented after normalization to GAPDH (n=4). Error bars indicate SEM. **statistically significant differences were defined as p<0.01 compared to vehicle treated wounds.

TNFα Expression

TNFα is primarily produced by neutrophils and macrophages during inflammatory phase of wound healing. Alone, TNF-α has been shown to inhibit wound re-epithelialization. The effects of exogenous TNF-α are dependent on concentration and duration of exposure emphasizing the importance of balancing the pro-inflammatory signals controlling wound healing. TNF-α, at low levels, can promote wound healing by indirectly stimulating inflammation and increasing macrophage produced growth factors. However, at higher levels, especially for prolonged periods of time, TNF-α has a detrimental effect on healing. TNF-α suppresses synthesis of extracellular matrix proteins and therefore affects granulation tissue formation.

Wounds treated with peptide 2605-4 had the highest expression of TNFα (**Figure 26**), in line with the induction of IL-1α and IL-8. In summary high expression levels of the evaluated pro-inflammatory cytokines observed in wounds treated with the peptide 2605-4 at day 10 support prolonged, unresolved inflammation and inhibition of wound healing as concluded by histopathology section above.

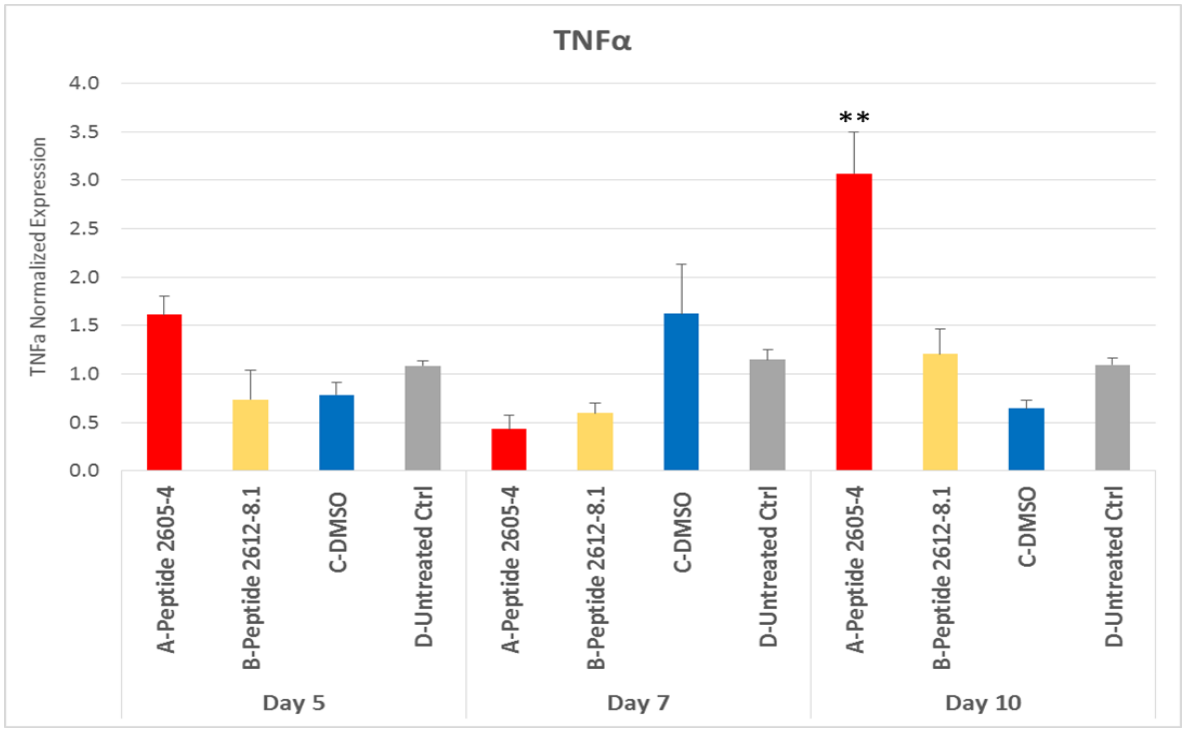

Figure 26. T**reatment with the peptide 2605-4 resulted in marked induction of TNFα at day 10.** Mean values of expression levels were represented after normalization to GAPDH (n=4). Error bars indicate SEM. **statistically significant differences were defined as p<0.01 compared to vehicle treated wounds.

The histopathology results and representative H&E staining of all treatment groups at day 10 further corroborate molecular analyses and prolonged inflammatory response in wounds treated with peptide 2605-4. Prolonged inflammation in wounds treated with 2605-4 may even contribute to partial tissue necrosis. More pronounced hematoxylin staining (purple) in wounds treated with peptide 2612-8.1 also suggests higher levels of inflammation corresponding to induced expression levels of IL-8 (**Figure 27**). Almost complete remodeling was observed in control untreated wounds, while tissue remodeling was still observed in the wound bed of DMSO treated wounds.

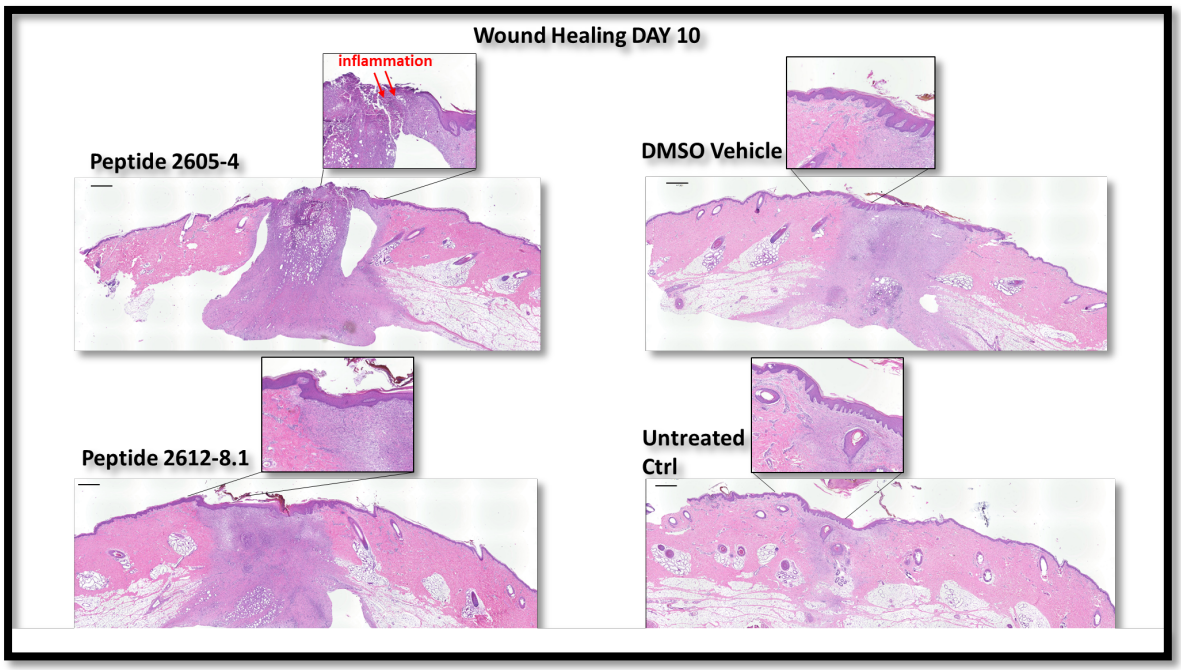

Figure 27. Representative histology of the full thickness wounds at the day 10. H&E images complementing histopathology report and molecular analyses of inflammatory response.

What opportunities for training and professional development has the project provided?

- *Nothing to Report*

a) **How were the results disseminated to communities of interest?**

Presented at the Military Health System Research Symposium, Kissimmee, FL, August 19-22, 2019 (Appendix 1)
Will be presented at SAWC/WHS meeting 2020

We are currently working on two manuscripts for the microbiology and wound healing evaluations.

Wound Healing Society: Concurrent Session:
Biofilms & Microbiomes
Friday April 15, 2016 2:15 p.m. − 3:15 p.m.
K3.01 - NOVEL CYCLIC LIPOPEPTIDES WITH ENHANCED ANTIBACTERIAL AND ANTIBIOFILM ACTIVITY AGAINST CHRONIC WOUND PATHOGENS
I. Pastar[1], B. Williams[2], J. Gil[1], J. Valdes[1], A. Higa[1], M. Solis[1], P. Cudic[2], S. C. Davis[1]
[1]University Of Miami Miller School Of Medicine, Dermatology And Cutaneous Surgery, Miami, FL, USA [2]Torrey Pines Institute For Molecular Studies, Port St. Lucie, FL, USA

Impact

a) **What was the impact on the development of the principal discipline(s) of the project?**
Nothing to Report

b) **What was the impact on other disciplines?**
Nothing to Report

c) **What was the impact on technology transfer?**
Nothing to Report

d) **What was the impact on society beyond science and technology?**
Nothing to Report

Changes/Problems

a) **Changes in approach and reasons for change**

One of the partnering PIs, Predrag Cudic left Torrey Pines and is at Florida Atlantic University. Dr. Richard Houghten (founder and CEO of TPI) took over as parterning PI.
Dr. Devore (Rutgers) who is subcontracted by Torrey Pines told us that he no longer has the funds to complete the last part of proposal.

b) **Actual or anticipated problems or delays and actions or plans to resolve them**

The major delay in this grant was that Dr. Cudic resigned from Torrey Pines Institute (TPI) and it took several months to transfer the grant to Dr. Richard Houghten (founder and CEO of TPI). Dr. Houghten has hired someone to perform the necessary work to complete the grant.
Since Dr. Devore was not able to complete his nanoformulation portion of the grant, we had to use DMSO as a vehicle. We found that the higher concentrations of peptides were able to obtain better efficacy.

Changes that had a significant impact on expenditures

Change of partnering PI at Torrey Pines has produced some delays in the in vivo evaluations, however we were successfully complete the proposed studies.

d) **Significant changes in use or care of human subjects, vertebrate animals, biohazards, and/or select agents**

Nothing to Report

e) **Significant changes in use or care of human subjects**

Nothing to Report

f) **Significant changes in use or care of vertebrate animals**

Nothing to Report

2. Significant changes in use of biohazards and/or select agents

Nothing to Report

3. Products

Abstract (see above) and two manuscripts will be submitted in the near future.

4. Participants & Other Collaborating Organizations

a) What individuals have worked on the project?

Name:	Stephen Davis
Project Role:	PI
Researcher Identifier:	
Nearest person month worked:	12 months
Contribution to Project:	Professor Davis is overseeing all of the in vivo studies and works Torrey Pines and coordinates the efforts of the collaborators.
Funding Support:	Not applicable

Name:	Joel Gil
Project Role:	Laboratory Manager
Researcher Identifier:	
Nearest person month worked:	12 months
Contribution to Project:	Joel Gil performs all surgery and

	treatments to the animals. He performs the assessments
Funding Support:	Not applicable

Name:	Jose Valdes
Project Role:	Research Assistant
Researcher Identifier:	
Nearest person month worked:	12 months
Contribution to Project:	Jose assists with all procedures on the animal. Performs animal monitoring.
Funding Support:	Not applicable

Name:	Michael Solis
Project Role:	Research Associate
Researcher Identifier:	
Nearest person month worked:	12 months
Contribution to Project:	Michael makes all microbiology media, assists with surgery and animal records
Funding Support:	Not applicable

Name:	Alex Higa
Project Role:	Research Associate
Researcher Identifier:	
Nearest person month worked:	12
Contribution to Project:	Alex assists will microbiology media, animal surgery and records
Funding Support:	Not applicable

Name:	Irena Pastar
Project Role:	Research Associate Professor
Researcher Identifier:	
Nearest person month worked:	12
Contribution to Project:	Perform the molecular virulence anlaysis
Funding Support:	Not applicable

Has there been a change in the active other support of the PD/PI(s) or senior/key personnel since the last reporting period?

The only changes involved a PI change and hiring of a new postdoc following the resignations of Dr. Cudic.

What other organizations were involved as partners?

Organization Name: Torrey Pines Institute
Location of Organization: Port St. Lucie, Florida
Partner's contribution to the project: Collaboration

Appendix 1: Presented at the Military Health System Research Symposium, Kissimmee, FL, August 19-22, 2019

Evaluation of cyclic lipopeptide formulations on the proliferation of Methicillin Resistant *Staphylococcus aureus* USA300 and *Pseudomonas aeruginosa* PA09-010 in a porcine full thickness wound model

Joel Gil*, Michael Solis*, Jose Valdes*, Alexander Higa*, Shruti Padhee[+], Heather Michaels[+], Brian Lenhart[+], Richard Houghten[+] Stephen C. Davis*. * Department of Dermatology and Cutaneous Surgery, University of Miami Miller School of Medicine, Miami, Florida,[+] Torrey Pines Institute for Molecular Studies, Port St. Lucie, Florida

Abstract:

Nosocomial infections are common in many healthcare provider settings, including military treatment facilities (MTFs). One of the common complications in forward operating bases (FOBs) or the battlefield is to maintain a sterile environment when applying treatment to open wounds[1]. Several pathogens require individualized antibiotic therapy engineered to target each specific bioburden[2]. Both Methicillin Resistant *Staphylococcus aureus* and *Pseudomonas aeruginosa* are difficult to treat and require their own respective treatment modality, such as Mupirocin and Silver Sulfadiazine[3]. A multi-targeting antibiotic can offer the medic or corpsman a readily-available method of intervention for an undiagnosed infection in the field[4]. The purpose of this study was to examine the effect of a novel cyclic lipopeptide that inhibits the proliferation for both MRSA and PA using a well-established *in vivo* porcine wound biofilm model. Four (4) pigs were wounded, each with thirty-six (36) full thickness wounds. 2 animals were inoculated with Methicillin Resistant *Staphylococcus aureus* (MRSA) USA300 and 2 with *Pseudomonas aeruginosa* PA09-010, all wounds covered with a polyurethane film dressing for 24 hours to allow biofilm formation. Wounds were then divided into four groups: DMSO + Peptide 2605-4 (20 mg/ml)* against MRSA or DMSO + Peptide 2612-8.1 (20 mg/ml)* against PA; DMSO Vehicle Control*; Mupirocin positive control; and compared to untreated control. Microbiological wound assessments were performed from four wounds on days 2 and 5 post infection. For both MRSA and PA analysis, the peptide exhibited comparable results against the respective positive control by day 2 while showing significantly ($p < 0.05$) lower results than baseline, untreated and Vehicle control wounds. Those wounds treated with DMSO + Peptide had bacterial reductions of at least 99.30% when compared against their respective baseline and untreated control groups. By day 5, MRSA infected wounds treated with DMSO + Peptide had bacterial reductions of at least 99.98% when compared against baseline wounds and untreated control. PA infected wounds treated with DMSO + Peptide were significantly ($p < 0.05$) lower than all other wounds, including the positive control. These results suggest that the lipopeptide can offer desirable benefits against biofilm infected wounds, both antibiotic resistant staph (MRSA) and/or *P. aeruginosa*. However, further testing evaluating the antimicrobial capacity having any effect, in favor or against, the wound healing process should be evaluated. These results may have significant clinical implications when treating infected wounds in military personnel in a hospital setting and battlefield.

* Torrey Pines Institute for Molecular Studies, Port St. Lucie, Florida
This study was supported by US Army grant W81XWH-15-1-0658

References

1. Mertz PM, Oliveira-Gandia MF, Davis SC. The evaluation of a cadexomer iodine wound dressing on methicillin resistant *Staphylococcus aureus* (MRSA) in acute wounds. Dermatologic Surgery 1999 Feb;25(2):89-93.
2. Roberts JA, Abdul-Aziz MH, Lipman J, et al. Individualized antibiotic dosing for patients who are critically ill: challenges and potential solutions. Lancet Infect Dis. 2014;14(6):498-509.
3. Davis SC, Ricotti C, Cazzaniga AL, Welch E, and Mertz PM. Microscopic and Physiological Evidence for Biofilm-Associated Wound Colonization *in-vivo* Wound Repair and Regeneration 2008; 16: 23-29.
4. Department of Defense Joint Theater Trauma System, Clinical Practice Guideline (Initial Management of War Wounds). Published: 24 April 2012.

Appendix 2: Will be presented at SAWC/WHS meeting 2020

Cyclic lipopeptide formulations effects on Methicillin Resistant Staphylococcus aureus USA300, Pseudomonas aeruginosa and wound healing using a porcine full thickness wound model

Joel Gil1, Predrag, Cudic2 , Michael Solis1, Jose Valdes1, Alexander Higa1, Jie Li1, Shruti Padhee 2, Heather Michaels 2, Brian Lenhart 2, Richard Houghten2 and Stephen C. Davis1.
1 Dr. Phillip Frost Department of Dermatology and Cutaneous Surgery, University of Miami Miller School of Medicine, Miami, Florida.
2 Department of Chemistry and Biochemistry, Florida Atlantic University
3 Torrey Pines Institute for Molecular Studies, Port St. Lucie, Florida

Abstract:
Chronic and acute wound infections can be difficult to treat and very costly.1 Cationic antimicrobial cyclic lipopeptides have been developed to provide broad spectrum activity.2 The purpose of this study was to examine the effect of two novel cyclic lipopeptides on wounds infected with either Methicillin Resistant Staphylococcus aureus (MRSA) or Pseduomonas aeruginosa (PA) using porcine infection models.3,4 We also determined their effect on healing. For the microbiology study (n=4), 36 full thickness wounds (10mm) were created. Two animals were inoculated with MRSA and the other two with PA. Prior to treatment all wounds were covered with a polyurethane film dressing for 24 hours to allow biofilm formation.3 Wounds were then divided and treated daily with either: DMSO+Peptide 2605-4 (20mg/ml) against MRSA or DMSO+Peptide 2612-8.1 (20mg/ml) against PA; DMSO Vehicle Control; Mupirocin or silver sulfadiazine positive controls; or untreated control. The wound healing study (n=2) were wounded and treated as described above. Microbiological assessments were performed on days 2 and 5 post infection. Histological wound assessments were performed blinded on days 5, 7 and 10. For both MRSA and PA analysis, the peptide exhibited comparable results against the respective positive controls while showing significantly lower counts than baseline, untreated and Vehicle control wounds. By day 5, MRSA infected wounds treated with DMSO+Peptide had lower bacterial counts when compared against baseline wounds and untreated control. PA infected wounds treated with DMSO+Peptide were significantly lower than all other wounds, including the positive control. Peptide 2605-4 significantly inhibited re-epithelialization as compared to DMSO and untreated controls. These results show that the lipopeptides can have different antimicrobial and wound healing effects. Therefore, it is important when studying the effects of antimicrobial therapies, one also needs to evaluate their effects on healing. This data may have important clinical implications.

This study was supported by US Army grant W81XWH-15-1-0658

References
1. Lindholm C, Searle R. Wound management for the 21st century: combining effectiveness and efficiency. Int Wound J. 2016 Jul;13 Suppl 2:5-15. doi: 10.1111/iwj.12623.
2. Bionda, N.; Fleeman, R.M.; de la Fuente-Núnez. C.; Rodriguez, M.C.; Reffuveille , F.; Shaw, L.N.; Pastar, I.; Davis, S.C.; Hancock , R.E.W ; Cudic, P. Eur. J. Med. Chem., 2016 ,108, 354-363.
3. Davis SC, Ricotti C, Cazzaniga AL, Welch E, and Mertz PM. Microscopic and Physiological Evidence for Biofilm-Associated Wound Colonization in-vivo Wound Repair and Regeneration 2008; 16: 23-29.
4. Gil J, Natesan G, Li J, Valdes J, Harding A, Solis M, Davis SC, Christy RJ. A PEGylated fibrin hydrogel-based antimicrobial wound dressing controls infection without impeding wound healing. Int'l Wound Journal, 2017, doi:10:1111/iwj.1291